CHAPTER 1

INTRODUCTIONS

1.1 Background of study

Since from the first piloted flight in 1903, and this year sets 110 years of milestone, the technological advancement in aviation field is astonishingly high. From propeller driven aircraft to supersonic jet engine cruisers, advancement in aviation field is getting more and more complex. The most advanced military organizations in the world today use unmanned aerial vehicle UAV for reconnaissance and also for combat mission (Karl R. Klingebiel, 2006). Fine tuning of UAVs leads to another usage for civil purpose. UVA now serves to niche market where they begin to embrace the usefulness into law enforcement, search and rescue, border patrol and agricultural (Newcome, 2004).

The limitation of UVA is its size, trouble brews when the need for going through tight space i.e., engineering equipment monitoring and search and rescue operation. In response to that Micro Air Vehicle (MAV) appeared in 1997 in response to DARPA program (C.thipyopas *et al*, 2011). Since then research have been carried to develop autonomous MAV capable of flying and hovering. Researchers are mostly in favor of propelled type flying object from single rotor to quad rotors, but there are some limitation associated to propel driven MAVs (T. Nick *et al*, 2001).

Since flying insects have excellent flying characteristic, researcher begin to develop biomimetic MAVs. Biomimetic MAVs must have a total wingspan less than 15cm and the flyer must be ornithopter (flapping wings) (H. Rajabi *et al*, 2011). The future potential of developed ornithopter is environmental monitoring, homeland security and for inspection of fragile or space limiting area.

Challenges associated with biomimetic (dragonfly) MAV is their flapping natural frequency starting at 19Hz to 37Hz depending on the species and the insects Reynold number is in the range of 100-10000 (Jiyu Sun *et al*, 2012). These figures pose a challenge together with relatively small size of MAV to develop a light weight yet strong and durable structure and materials for the wings

Biological pattern that can be found on the surface amongst flora and fauna leads to a curiosity of why would the pattern is shaped and what governs them. For example, dragon fly wing membrane has a complex geometry pattern on its surface (Jiyu Sun *et al*, 2012). Those geometry must be in that particular shape for a reason i.e. to improve its strength, aerodynamic or reliability.

1.2 Objective

Inspired from biomimetic units, this research was conducted in favor of materials for MAV wing membrane The objective of this research is to analyze the mechanical properties of PVA film with three unique biomimetic patterns named grid, striation and spot that will be drawn on the surface of the film. The main objective of this research is:

1. To prepare PVA thin film with different biomimetic pattern using heated geometry cutter.
2. To study the influence of biomimetic units to the mechanical properties of PVA thin film in terms modulus, tensile strength and elongation.
3. To analyze the effect of biomimetic units to the trend of loss modulus, storage modulus and Tangent Delta of thin film PVA in variable frequencies form 10Hz to 270Hz.
4. To measure the percentage of crystallization of PVA thin film with biomimetic units.

The data obtained were then compared among the three unique patterns and a non pattern (control) sample in terms of mechanical properties and mechanical behavior during variable frequencies.

1.3 Scope of study

This study was conducted in favor of materials competence for MAV wing membrane and the introduction of bio-units to the surface of the membrane.

Unique biomimetic units were drawn using heated geometry cutter onto the casted polyvinyl alcohol PVA thin film. Mechanical properties were evaluated using tensile testing machine and dynamic mechanical analyzer was used to evaluate the influence of variable frequencies on the mechanical properties. Percentage of crystallization was

measured using differential scanning calorimenty and physical examination was performed using optical microscope.

1.4 Problem statement

Mechanical properties of the MAVs wing membrane must be extraordinarily high without having a higher density. Addition of foreign particle to the thin film membrane increases the density of the membrane, thus contributing to the overall weigh which is not good for MAVs. The dragonfly wings has all the favorable characteristics a MAV needs, such as small size and the ability to hover and accelerate quickly both from dead stop as well from a hovering attitude.

However, the delicate wings have numerous structural cells that would make the wing relatively heavy for MAV flight and difficult to replicate. If reproduced mechanically, the biomimetic wings is always simplified or tailored for the needs only. This simplification can be enhanced by drawing a unique biomimetic pattern to elevate the mechanical properties based on the requirements.

CHAPTER 2

LITERATURE REVIEW

2.1 Polyvinyl alcohol PVA

Polyvinyl alcohol was first prepared by Hermann and Haehnel in 1924 by hydrolyzing polyvinyl acetate in ethanol with potassium hydroxide (S.K.Saxena, 2004). PVA is produced commercially from polyvinyl acetate, by continuous process. The acetate groups are hydrolyzed by ester interchange with methanol in the presence of anhydrous sodium methylate or aqueous sodium hydroxide. The physical characteristics and its specific functional uses depend on the degree of polymerization and the degree of hydrolysis. Polyvinyl alcohol is classified into two classes namely: partially hydrolyzed and fully hydrolyzed.

Polyvinyl alcohol is an odorless and tasteless, translucent, white or cream colored granular powder. It is used as a moisture barrier film for food supplement tablets and for foods that contain inclusions or dry food with inclusions that need to be protected from moisture uptake. Polyvinyl alcohol is not known to occur as a natural product.

Polyvinyl alcohol has excellent film forming, emulsifying and adhesive properties. It has high tensile strength and flexibility. But those properties are dependent on humidity, because in this experiment, PVA solution is achieved by solvent casting by mixing hydrolyzed PVA powder and distilled water. Higher the humidity, more water is absorbed and PVA film will exhibit more ductility properties and reduced tensile strength.PVA is fully degradable and dissolves quickly. PVA has a molecular formula of $(C_2H_4\ O)_X$. Figure 2.1 shows the structure of polyvinyl alcohol (partially hydrolyzed).

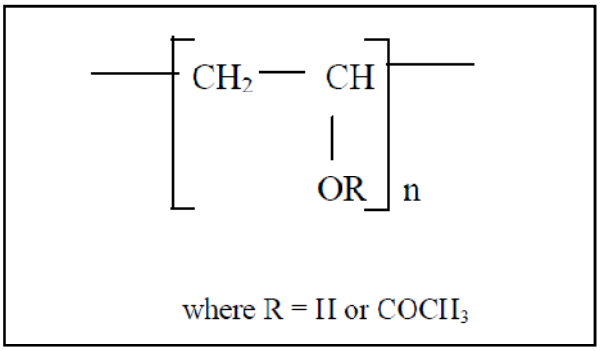

Figure 2.1: Structure of polyvinyl alcohol

Table 2.1 shows the typical properties of polyvinyl alcohol (S.K.Saxena, 2004). PVA is commonly used in medical devices due to its low protein adsorption characteristics, biocompatibility, high water solubility, and chemical resistance. The polyvinyl alcohol has many uses in the ceramics industry as temporary binders and plastifying agents. They are suitable for processing various raw materials, such as china mixes, oxide ceramic mixes, metal powders and ferrites. The applications range from household ceramics including the production of tableware, to technical ceramics, such as the production of ignition plugs or insulators.

Table 2.1 Properties of polyvinyl alcohol

pH	5.0-6.5
Melting point	180-190°C
Molecular weight	26300-30000
Degree of hydrolysis	86.5-89%
Density	1.19-1.39 g/cm^3

2.2 Solvent casting

The continuous solvent casting process is one of the oldest in plastic film manufacturing. It was developed more than hundred years ago driven by the needs of the emerging photographic industry. Nowadays, the solvent cast technology is becoming increasingly attractive for the productions.

The key element for a simple solvent casting is (Ulrich Siemann, 2005):

1. The polymer must be soluble in a volatile solvent or water
2. A stable solution with a reasonable minimum solid content and viscosity should be formed
3. Formation of a homogeneous film and release from the casting support must be possible.

To provide these properties many process tricks are used such as co-solvent systems, dissolution at overpressure, use of special molecular weight distributions of polymers or co-polymers, additives such as plasticizers, release agents etc.. Starting with

the cellulose derivatives used from the historical beginning of this technique, processes for other high performance materials have been developed over the last 40 years. Water is still a common solvent for food-grade films made of biopolymers or polyvinyl alcohol. Typical additives used to provide specific film properties are anti blocking and antistatic compounds, chelating agents, colors, electrical conductive substances, pigments etc.

2.2.1 Advantages and disadvantages

Solvent casting is simple yet an efficient way for producing thin film polymer. The main advantage of solvent cast is due to the drying method that does not require any external mechanical force or thermal stress.

Advantages are (Ulrich Siemann, 2005) :

1. Homogeneous thickness distribution
2. Highest optical purity, free of gels or specks
3. Excellent transparency, low haze
4. Isotropic orientation, low optical retardation, excellent flatness
5. Processing of thermally or mechanically sensitive components is feasible
6. Possibility of production of high-temperature resistant films from non-melting but soluble raw materials

There are constraints on the types of polymer films for which solvent casting technology must or cannot be used. Relatively few materials can be processed into films by both methods – slot extrusion and solvent casting. In these cases, a cost-performance

comparison decides. Very thin films cannot be produced by extrusion without stretching and very thick films are very costly to produce by solvent casting and lamination. In general, solvent-cast products are more expensive than extruded film to manufacture for several reasons:

1. Slow production speed depending on a slow solvent diffusion process
2. Extra energy costs of solvent recovery
3. Investments in facilities for handling solvents and dope solutions

On the other hand, the performance and, more specifically, the high quality of solvent cast films cannot be achieved using other processes.

2.2.2 Process and application

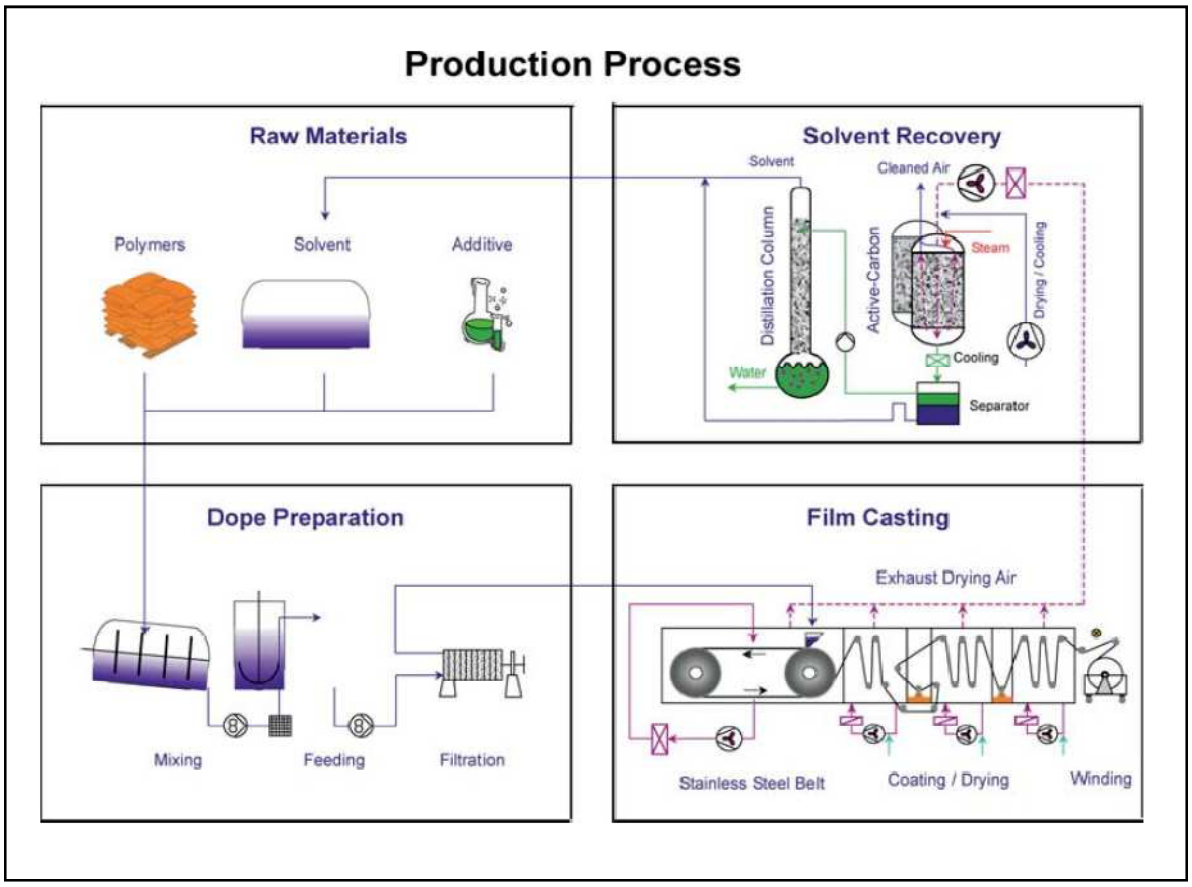

Figure 2.2: Solvent casting process

Figure 2.2 shows the typical solvent casting process. The usage of solvent casting film accelerates with the film industries where the demand for thin film increases. In the case of PVA, LCD application uses solvent casting technology to cast PVA film for polarizing function. Other advantages of cast film technology are important for electrical and electronic applications. Electrical properties that are stable at high temperatures over the long term can only be achieved with polymers with high or no melting temperatures. It is often not feasible to produce these films using thermoplastic manufacturing methods. Therefore industrialist opted to use solvent casting technologies.

2.3 Biomimetic units

Rigorous research have been carried out to improve mechanical property of a metallic and non metallic material i.e. polymer to meet the higher requirements practical usage. Adding foreign particle such as fiber and nano particle to a polymer substance does improve the mechanical property dramatically but the plastic deformation capabilities were jeopardized in exchange for an increase toughness and strength. Therefore a research is needed from a different point of view to increase both toughness and plastic capabilities in polymer without adding any foreign particle.

Research has been conducted on biomimetic units to improve the wear resistance of compact graphite cast iron (CGI) with biomimetic units on the surface. The wear behaviors of biomimetic specimens as functions of laser input energy and biomimetic unit shape were investigated and the results indicated that the biomimetic specimens had better wear resistance than the untreated specimens (Hong Zhou *et al*, 2007).

Researcher found that, there are three basic typical structural shapes of natural biomimetic units with excellent biomechanical properties against the environment they are called “striation”, “spot” and “gridding” (Chuanwei Wang *et al*, 2013).

2.3.1 Striation

Striation shaped units are the one found in tree leaf. Figure 2.3 below shows striation shape units on a leaf.

Figure 2.3: Striation shape on a leaf

Tree leaves have an excellent characteristic for water repellant and high toughness and the shape geometry place a major role in determining the mechanical property of a leaf. Some unique structures of plants leaves have been formed in evolutionary process of adapting to environments, showing excellent mechanical characteristics. The studies on these unique structures may offer references for structure designs in engineering area. Halyk *et al.* (1968) made an inchoate research on the tensile and shear strength characteristics of alfalfa stems. Zebrowski. (1999) investigated the kinematic and dynamic attributes and their interrelations in freely swaying in florescence-bearing stems of wheat and triticale, and established a model of static stem bending resistance. Ahmad *et al.*(2005) investigated mechanical strength and bending characteristics of bamboo.

2.3.2 Spot

Spot shaped units are the one found in ground beetle. Figure 2.4 below shows spot shaped unit on the wing of ground beetle.

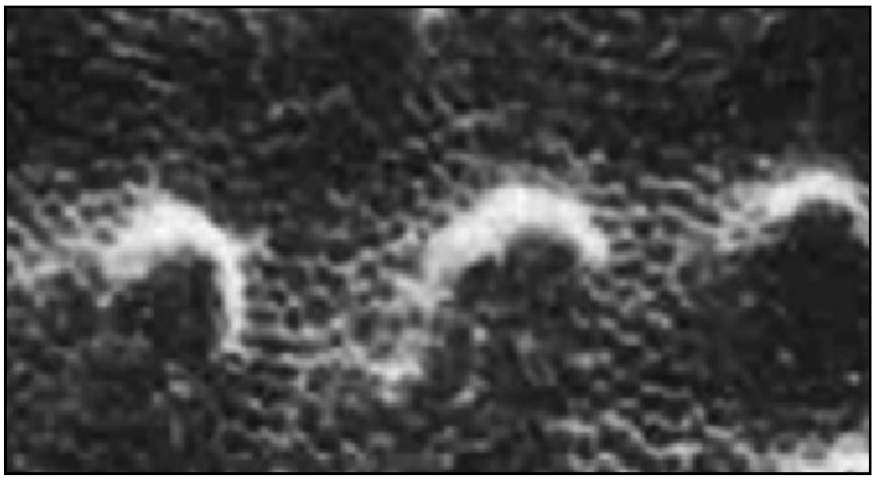

Figure 2.4 Spot shapes on a ground beetle

Natural biomaterials have some special structures and functions. The skeleton of insect cuticle, as an excellent crude composite material, is tenacity, waterproof and lightweight. The insect cuticle has evolved for a variety of demanding duties, such as flying, digging and swimming. Insect cuticle possesses excellent mechanical properties, such as strength, stiffness and fracture toughness. The structures of insect cuticle have been analyzed by researchers (Wegst *et al*, 2004). It is shown that the cuticles surface of dung beetle has a laminative composite structure. Peng X H *et al*, (2000) summarized the types of arrangement of plies, and found that different types of arrangement exhibit different properties. Based on the dual helicoidal arrangement of plies of insect cuticle, biomimetic composite plies were fabricated and the fracture toughness was increased by 13.7% compared with that of conventional ones.

2.3.3 Gridding

Grid shape is the one found in dragonfly wings. Figure 2.5 below shows grid shaped unit on dragonfly wings.

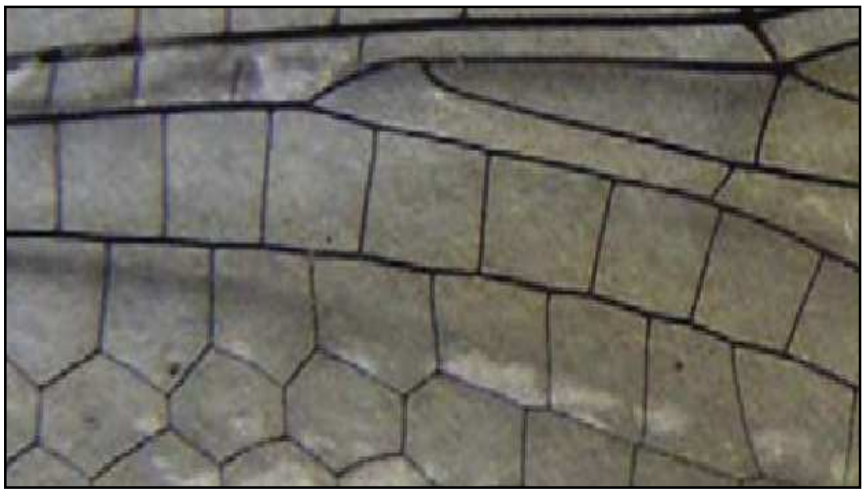

Figure 2.5: Gridding shape on dragonfly wings

Scientists have been intrigued by the dragonfly wings structure and have carried out research for biomimetic applications. Relative to the large number of works on its flight aerodynamics, few researchers have focused on the insect wing structure and its mechanical properties. The wings of dragonflies are mainly composed of veins and membranes, a typical nanocomposite material . The veins and membranes have a complex design within the wing that give rise to whole-wing characteristics which result in dragonflies being supremely versatile, maneuverable fliers. The wing structure, especially corrugation, on dragonflies is believed to enhance aerodynamic performance (Jiyu Sun *et al*, 2012)

Dragonfly wings are composed of a thin cuticular membrane that is supported by a system of veins. The veins are hollow branching tubes that form the supporting framework, which often have cross-connections that form closed "cells" within the membrane (extreme examples include *Odonata* and *Neuroptera*) (J.G. Needham 1903).

Researcher investigated different positions of a dragonfly cuticle using a nanoindenter, and the calculated moduli values are 4.7 ± 0.6 GPa, 2.9 ± 0.8 GPa, 1.5 ± 0.5 GPa for the dry body cuticle (abdominal tergite), dry wing veins, and wing membrane, respectively (M. Kempf. 2000). It demonstrates that the moduli of wing veins are larger than that of the membrane. It is supposed that the vein is the main load-bearing part.

2.4 Research on biomimetic units

Research had been conducted by (Zhihui Zhang *et al*, 2010) where tot work tool steel under annealed condition, AISI H13, was used to study the influence of biomemetic units imprinted on the specimen. The effect of thermal fatigue cycling on the tensile properties of H13 die steel specimens with different surfaces (several types of biomimetic surfaces and a smooth surface) was compared and investigated.

Tensile tests at room temperature showed that biomimetic specimens exhibited remarkably enhanced UTS and YS as compared with specimens with smooth surface, while corresponding ductility was almost not affected even heightened after thermal fatigue loaded. The different requirements for strength and ductility depend on the morphological features on the biomimetic surface such as the arranging direction, spacing and shape of units, as well as the laser parameters which contribute to the unit size and inside

microstructure characteristics. The increased comprehensive mechanical property of biomimetic specimens is the result of coupling effect that involves the morphological features on the surface and the microstructure characteristics within the units.

Chuanwei Wang investigated the tensile property of hot work tool steel prepared by biomimetic coupled laser remelting process with different laser input energies (Chuanwei Wang *et al*, 2012). Hot work tool steel (4Cr5MoSiV1) was manufactured using a laser with different input energies. Results of tensile tests confirmed that the biomimetic peg shape units coupled laser remelting (BCLR) process had an advance effect on improving the strength and ductility of 4Cr5MoSiV1 steel simultaneously.

Microstructure examinations demonstrated that a fine microstructure along with nano scale carbide was acquired in the BCLR units, which produced an accumulative contribution of grain refinement, precipitation strengthening and a mixed microstructure. The BCLR method resulted in a marked improvement in the strength and ductility of 4Cr5MoSiV1 steel simultaneously. There is an optimal laser input energy (160 J/cm2, BCLR-3) contributes maximal increment in tensile property, and further increasing the input energy (205 J/cm2, BCLR-4) results in tensile property deterioration related mainly to the severe depressions on the units.

Hong Zhou *et al*, (2007) investigated wearable characteristic surface of cast iron with biomimetic units processed by laser .An attempt to improve the wear resistance of compact graphite cast iron (CGI) with biomimetic units on the surface was made by using a biomimetic coupled laser remelting (BCLR) process. The microstructure and microhardness of biomimetic units were examined. The wear behaviors of biomimetic specimens as functions of laser input energy and biomimetic unit shape were investigated

under dry sliding condition, respectively. The specimen with grid biomimetic units had the best resistance, the stria took the second place and the convex showed the worst.

Wear tests show that the bio-inspired wearable surface can improve the wear resistance of CGI sliding against GCr15 steel rings under dry sliding condition. Both the laser input energy and the shape of biomimetic units influence the wear resistance of the biomimetic specimens. Along with the increase of laser input energy, the depth, the width and the hardness of the biomimetic unit increase, so does the wear resistance. Concerning the shapes of the biomimetic unit, the grid shape biomimetic specimen exhibits the best wear resistance among the three kinds of the biomimetic specimens, the stria times, and the convex worst.

Chuanwei *et al*, (2013) investigated the effects of biomimetic units on the surface of low carbon steel. An attempt to improve the mechanical property of low carbon steel with biomimetic units was made by using a laser remelting process. Three kinds of shapes including ‘striation’, ‘spot’ and ‘gridding’, were chosen for forming the biomimetic units. Microstructure and microhardness examinations demonstrated that desirable microstructural changes and regular hardness distribution were acquired in the units..

It was found that the biomimetic method resulted in a marked improvement in the strength and ductility of S355 steel simultaneously. Factors, such as the desirable microstructure changes in the units and the stress redistribution derived from efficient stress transfer are the main reasons for enhancing the mechanical property of S355 steel with biomimetic units. Biomimetic samples with different unit shapes showed different tensile behavior. Two dimensional biomimetic units contribute to the enhancement of strength and ductility simultaneously, while one dimensional biomimetic units contribute mainly to the enhancement of strength. By comparison, continuously distributed units have more beneficial influence on the enhancement of tensile property than the discontinuous units do.

The main advantage of the biomimetic process is the ability to enhance the strength and ductility of materials simultaneously without changing the special properties of substrate materials. Moreover, compared with other chemical or physical methods, this process has the following advantages: composition purity, controllable parameters and simple procedures.

2.5 Tensile testing

A tensile test is the most basic type of mechanical that can be performed on material. Tensile tests are simple, inexpensive, and standardized for quality purpose. The principle is by pulling a specimen by a fixed clamp on one end and a moving clamp on the other end. The machine will determine how the material will react to forces being applied in tension. As the material is being pulled, the strength along with elongation can be calculated.

A curve will be displayed showing how it reacted to the forces being applied. The point of failure is of much interest and is typically called "Ultimate Strength" or UTS. Figure 2.6 shows a typical stress strain curve.

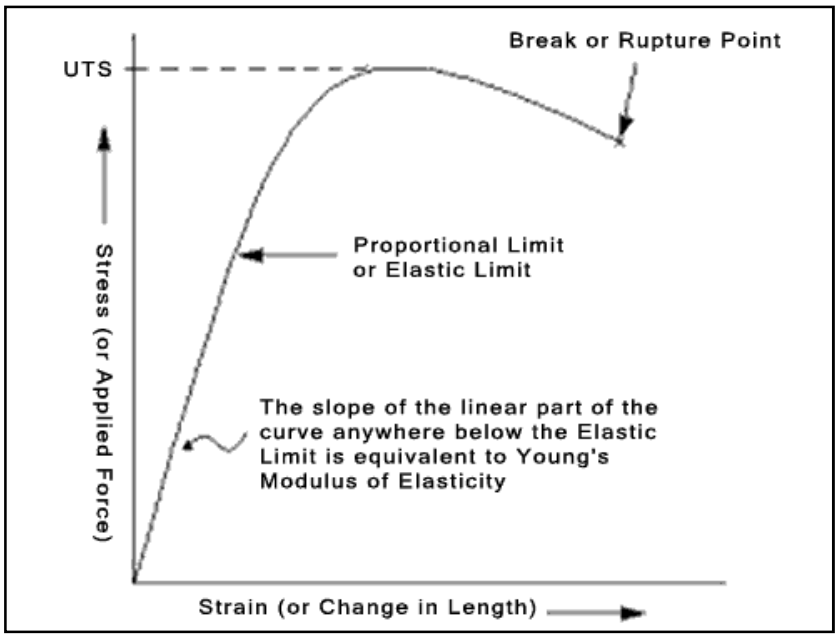

Figure 2.6 Stress strain curve (UTS)

2.5.1 Hooke's Law

For most of the tensile testing, the initial portion of the test, the relationship between the applied force, or load, and the elongation the specimen exhibits is linear. In linear region, the line obeys the relationship defined as "Hooke's Law" where the ratio of stress to strain is a constant, or $\frac{\sigma}{\varepsilon}$=E is the slope of the line in this region where stress (σ) is proportional to strain (ε) and is called the "Modulus of Elasticity" or "Young's Modulus".

2.5.2 Modulus of Elasticity

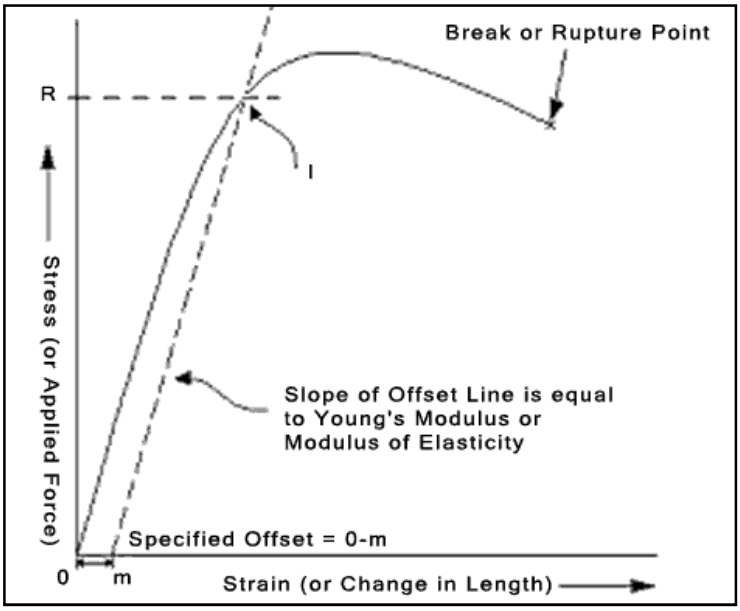

Figure 2.7: Modulus of elasticity

The modulus of elasticity is a measure of the stiffness of the material, but it only applies in the linear region of the curve as can be seen from figure 2.7. If a specimen is loaded within this linear region, the material will return to its exact same condition if the load is removed. At the point that the curve is no longer linear and deviates from the straight-line relationship, Hooke's Law no longer applies and some permanent deformation occurs in the specimen. This point is called the "elastic, or proportional, limit". From this point on in the tensile test, the material reacts plastically to any further increase in load or stress. It will not return to its original, unstressed condition if the load were removed.

2.5.3 Yield Strength

A value called "yield strength" of a material is defined as the stress applied to the material at which plastic deformation starts to occur while the material is loaded.

2.5.4 Strain

The amount of stretch or elongation the specimen undergoes during tensile testing can be expressed as an absolute measurement in the change in length or as a relative measurement called "strain". Strain itself can be expressed in two different ways, as "engineering strain" and "true strain". Engineering strain is probably the easiest and the most common expression of strain used.

2.5.5 Ultimate Tensile Strength

Ultimate tensile strength (UTS) is the maximum load the specimen sustains during the test. The UTS may or may not equate to the strength at break. This all depends on what type of material that are being tested.

2.5.6 ASTM D 882

ASTM D882 covers the determination of tensile properties of plastic in the form of thin sheeting for a film less than 1mm thickness. The test specimen width and thickness should be at least 50mm longer than the grip separation and the nominal width of the specimen should not be less than 5.0mm or greater than 25.4mm with a width thickness ration of 8 or greater (ASTM vol 8).

2.6 Dynamic Mechanical Analysis

Dynamic Mechanical Analysis, DMA is a measurement tool that is widely used to characterize a material's properties as a function of temperature, time, frequency, stress, atmosphere or a combination of these parameters.

DMA is a technique where a small deformation is applied to a sample in a cyclic manner. By doing this, the material response to stress, temperature, frequency and other values can be studied. DMA is also called DMTA for Dynamic Mechanical Thermal Analysis.

DMA works by applying a sinusoidal deformation to a sample of known geometry. The sample can be subjected by a controlled stress or a controlled strain. For a known stress, the sample will then deform a certain amount. In DMA this is done sinusoidally. The

deformation of the sample depends of the stiffness of the material used. A force motor is used to generate the sinusoidal wave and this is transmitted to the sample via a drive shaft.

DMA measures stiffness and damping, these are reported as modulus and tan delta. Since DMA machine applies sinusoidal force, the modulus can be express as an in-phase component, the storage modulus, and an out of phase component, the loss modulus, see Figure 2.8. The storage modulus, either E' or G', is the measure of the sample's elastic behavior. The ratio of the loss to the storage is the tan delta and is often called damping. It is a measure of the energy dissipation of a material (Kevin Menard. 2008).

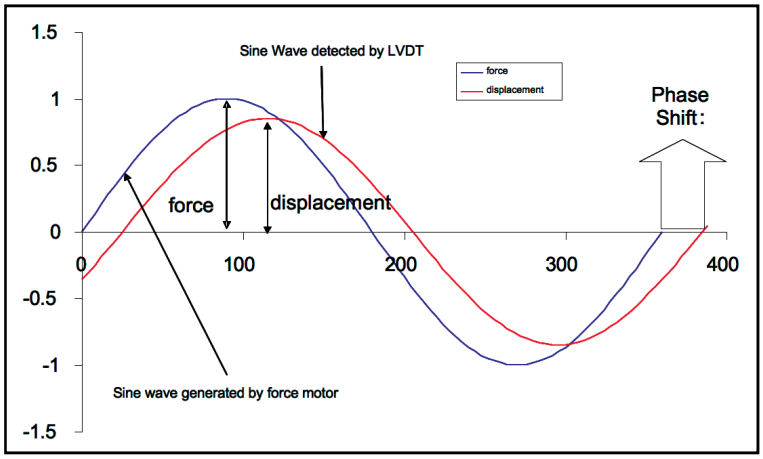

Figure 2.8 Graph generated from DMA machine

Two main properties that can be derived from DMA analysis is Loss modulus and Storage modulus. Loss modulus is a measure of the viscous response of a material. Also called the imaginary modulus or out of phase component. Storage modulus is a measure of the elastic response of a material but not the same as Young's modulus. It is also called the in-phase component (Montgomery Shaw *et al.* 2005).

2.7 Differential scanning calorimetry

Differential Scanning Calorimetry, or DSC, is a thermal analysis technique relating on how a material's heat capacity (Cp) is changed by temperature. A sample with a known mass is heated or cooled and the changes in its heat capacity are tracked as changes in the heat flow. This allows the detection of transitions like melts, glass transitions, phase changes, and curing.

The percentage of crystallization of a given polymer specimen can be calculated from the area under the graph of endothermic dip. Figure 2.9 shows the typical dsc curve. Crystallization can be calculated through the endothermic dip (Tc).

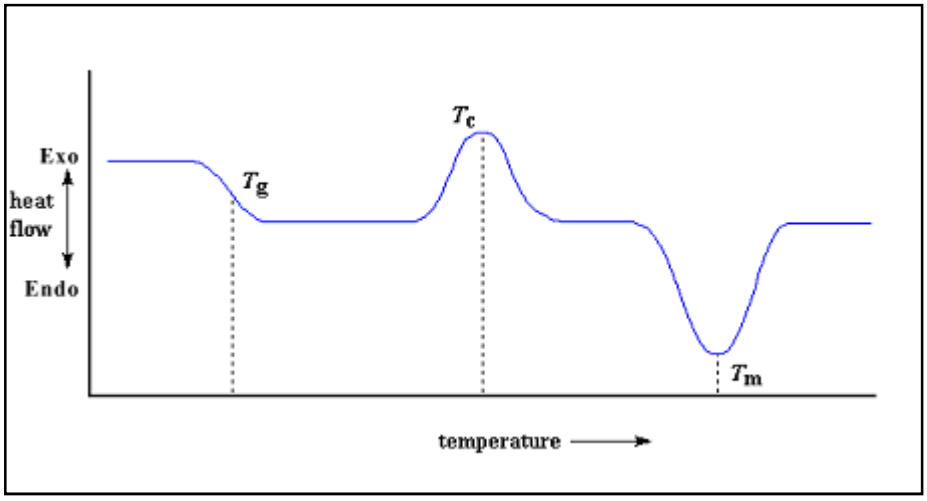

Figure 2.9: Typical plot for DSC

CHAPTER 3

METHODOLOGY

3.1 Introductions

Research methodology is all about the description on how the experiment is being conducted. An international standard process of methodology is important to ensure the validity and quality of the experiment being conducted and it does affect the end result of the experiment. For this project, there are six major part of methodology being used, namely Sample preparation, sample cutting, tensile testing method, DMA testing, optical microscope inspection and differential scanning calorimetry DSC testing.

3.2 Preparation of PVA, Polyvinyl alcohol

Solvent casting technique was implemented for the preparation of polyvinyl alcohol. Four trials were done to achieve the desired result. The first three trials were failed due to excess bubbles, warpage, and difficulties in removing the mold from the glass Petri dish.

The forth trial resulting in a complete success in preparing a thin film polyvinyl alcohol. The dimension used was 16cm (L) X 2.5cm (W) and thickness were controlled in a scale of 2.5mm+/- 0.1mm using vernier caliper. Polyvinyl alcohol powders from Kuraray Co. LTD were used. The specification is listed in table 3.1 below

Table 3.1: PVA specification

Type	Viscosity (Mpa)	Hydrolysis %max	Volatile %	Ash %	pH
PVA-220S	27-33	87-89	5.0	0.4	5-7

10g of polyvinyl alcohol were slowly added to 90g of distilled water (10wt) to avoid any lump formation. The solutions were weighted using AND model no GR-200 micro weightier. Motorized stirrer was used to stir the solution for at least 2 hours until PVA power dissolves in distilled water at room temperature. Once the powder is fully dispersed, the mix is heated at 90°C for 1 hour until PVA is fully solubilized. The solutions were casted in a Petri dish using funnel to remove access bubble and Aluminum foils were used as a mold layer to prevent solidified PVA from sticking on the glass Petri dish. Samples were cooled to using room temperature for 5 days in a dry cabinet condition.

3.3 Preparation of Polyvinyl alcohol film shape for tensile testing and DMA analysis

The dumbbell shaped specimens were cut from molded PVA thin film using type D Die T cutter. Figure 3.1 illustrates the dimension. Average thickness taken from three points from the gauge length is 0.45mm +/- 0.1mm

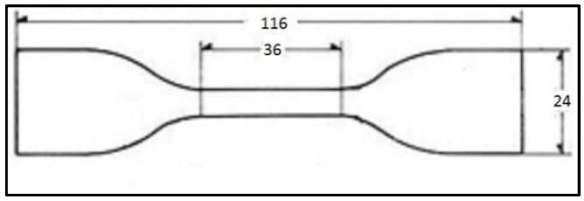

Figure 3.1: Dimension of PVA sample

3.3.1 Sample preparation for tensile testing

Four batches of samples with three specimens each were designed based on the structural shapes units in biological composition namely:

A: Striation —

B: Grid ⧺

C: Spot :::::

D: Plain ▭

A geometry cutter with a diameter of 0.2mm and depthness of 0.16mm were used to draw the corresponding pattern. Since polyvinyl alcohol is transparent, the drawing of the

pattern was relatively easy. Standard patterns with exact dimension were drawn in a piece of paper using pencil. Samples were rested on the pattern paper and both ends were tied using masking tape to ensure proper cutting performance. The blade tip was heated for 5sec interval using candle light. The patterns were designed such that it is symmetry to the gauge dimension i.e. no dimension irregularities on the gauge length. Figure 3.2 illustrates the samples with unique pattern drawn into it. Table 3.2 shows the detail dimension of the biomimetic units.

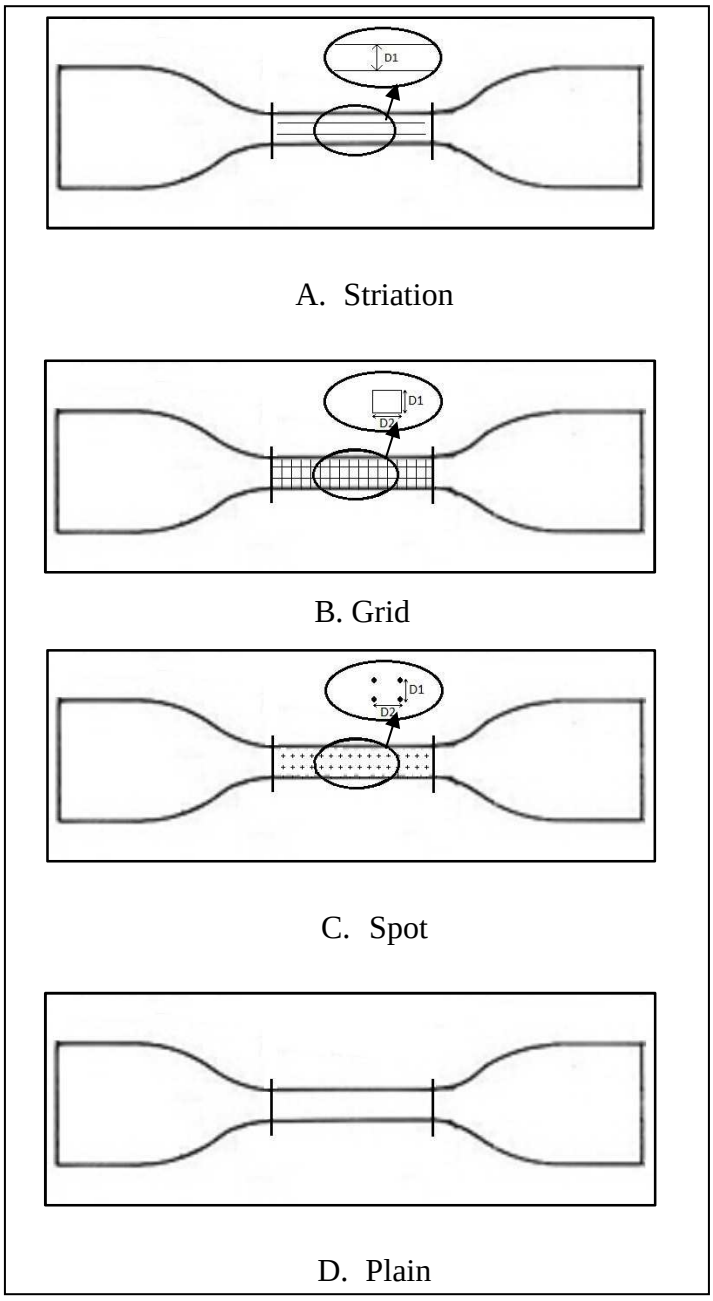

Figure 3.2: Biomimetic sample dimensions

Table 3.2: Biomimetic units dimension details.

Pattern	D1 (mm)	D2(mm)	Diameter(mm)
A (Striation)	2	N/A	0.2
B (Grid)	2	3	0.2
C (Spot)	2	3	0.2
D (Plain)	N/A	N/A	N/A

3.3.2 Sample preparation for Dynamic Mechanical Analysis testing

For Dynamic Mechanical Analysis testing, samples were outsourced to Mettler Toledo instrument supplier. The tests were performed using Mettler Toledo DMA 1 analyzer. Temperature was set at room temperature. Tension type of test was performed.

Four samples grid, striation, spot and plain with a dimension of tensile testing gauge length of 36mm and thickness of 0.34mm which were taken as an average from 3 point inside the gauge length from digital vernier caliper.

3.3.3 Sample preparation for differential scanning calorimetry testing

For DSC analysis, sample pan with approximately 5g of individual biomimetic samples were used to perform the test. Mettler Toledo DSC 820 was used to analyze the percentage of crystallinity.

For grid specimen, the cross unit were used as a sample since it denotes the grid shape perfectly. For striation two parallel lines were cut and taken as a sample. For dotted sample, a unit dot sample were cut and used as a sample. As for no pattern (control) specimen, there is no restriction on sample since there is no biomimetic units drawn.

3.3.4 Optical microscope

A optical microscope were used to observe formation of biomimetic units on each sample. The microscope is located in UMs ceramic lab. The system consists of the microscope itself and software which is used to analyze the image acquired.

3.4 Experiment parameters

The present study was initiated to investigate the influence of Biomimetics units on the mechanical property of polyvinyl alcohol PVA thin film inspired for Micro Aerial vehicle MAV wings material.

Parameters setup for tensile testing is Modulus at 0% stain (MPa), modulus at 100% strain (MPa), Maximum % of strain, Ultimate tensile strength (MPa) and Break strength (MPa). These parameters were intended to evaluate the basic mechanical property. ASTM D882 tensile testing method for thin film polymer was implemented for PVA tensile test.

Tensile properties were determined according to ASTM D882 standard at room temperature using universal testing machine, Instron model 3345 with 100N load cell and a crosshead speed of 10mm/min.

Micro Aerial Vehicle wings will be subjected to various frequencies during its service. The material behavior with different range of frequency under fixed strain can be evaluate using Dynamic Mechanical Analyzer DMA. Parameter setup for DMA is Storage Modulus (MPa), Loss Modulus (MPa) and Tangent Delta which would determine the mechanical characteristic under fixed room temperature with variable frequencies. Specimens were tested at variable frequency raging form 10Hz to 270Hz with a strain displacement of 10µm.

The percentage of crystallization can be found through DSC analysis. Since heated geometry cutter blade was used to draw the pattern on the specimen, additional crystal might be formed through sudden point heating and cooling along the pattern drawn i.e. grid, striation and spot. Those crystals are highly depends on the density of the pattern on the test gage, as the more closely pack, the more crystal formation would be. Temperature range of 30°C to 300°C with a increment of 10°C every minutes were used to test the PVA thin film. Glass transition temperature, meting temperature and percentage of crystallization can be obtained through this test. However only crystallization formation were studied using DSC.

CHAPTER 4

RESULT AND DISCUSSION

4.1 Introductions

Three unique biomimetic units, grid, striation and spot were drawn on the surface of casted PVA thin film. The patterns drawn were examined using optical microscope for structural integrity. Mechanical properties by means of tangent modulus, ultimate strength, break strength and maximum displacement were determined and the influence of the pattern on the mechanical properties was discussed. Stiffness and damping characteristic were measured using Dynamic Mechanical Analysis DMA in terms of loss modulus, storage modulus and tangent delta. The percentage of crystallinity was reported through Differential Scanning Calorimetry.

4.2 Optical microscope

The structural integrity of grid, striation and spot biomimetic units were examined using optical microscope with a magnification of 20X. Single units of pattern were found to be almost in proper geometry as required.

Figure 4.1 shows grid specimen. The cross pattern can be seen in the left edge of the picture. The average width of the grid pattern was 0.1mm. Crystals can be clearly seen along the width of the grid pattern. 36 grid boxes with 2cm width and 3cm length were drawn on the gage length of the specimen.

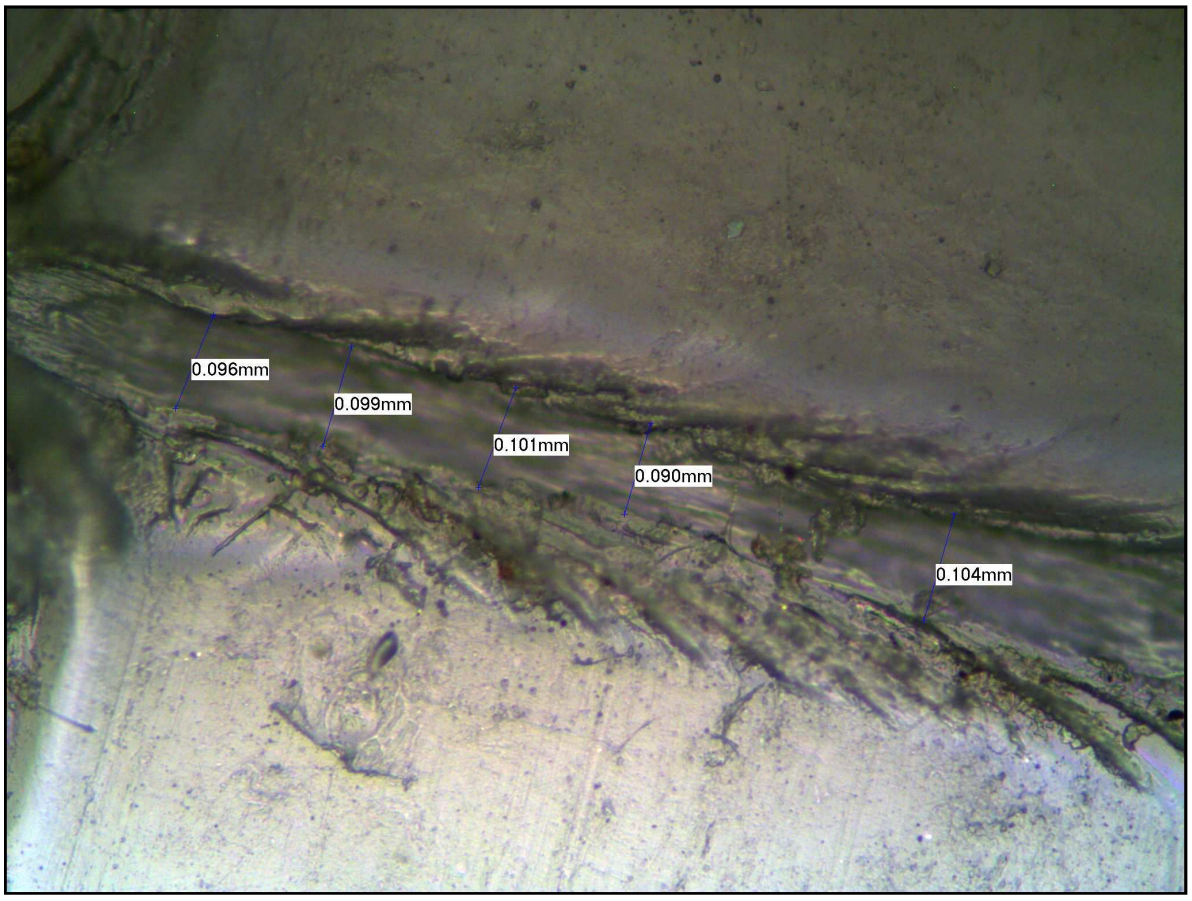

Figure 4.1: Image of grid specimen at 20X magnification

Figure 4.2 shows spot specimen. Due to heat localized heat of the cutter, crystals were observed around the circumference of the spot. Typical diameter of the spot units was 0.212mm. 26 spots were drawn on the specimen gage length depicted from the intersection of the grid pattern.

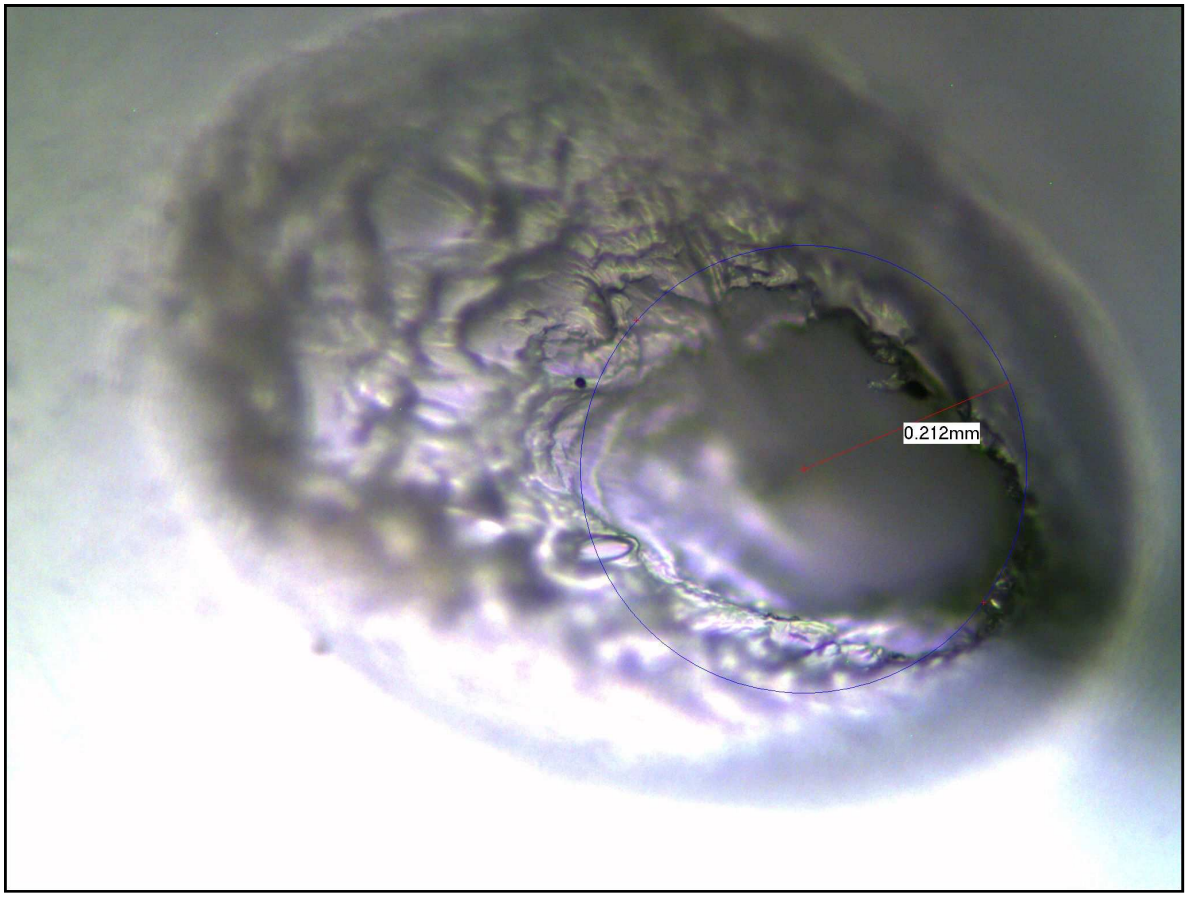

Figure 4.2: Image of spot specimen at 20X magnification

Striation shapes have two parallel lines running along the gage length. Figure 4.3 shows the striation specimen. The average width of the pattern was 0.1mm. Also crystal formation can be clearly seen on both edges on the pattern drawn.

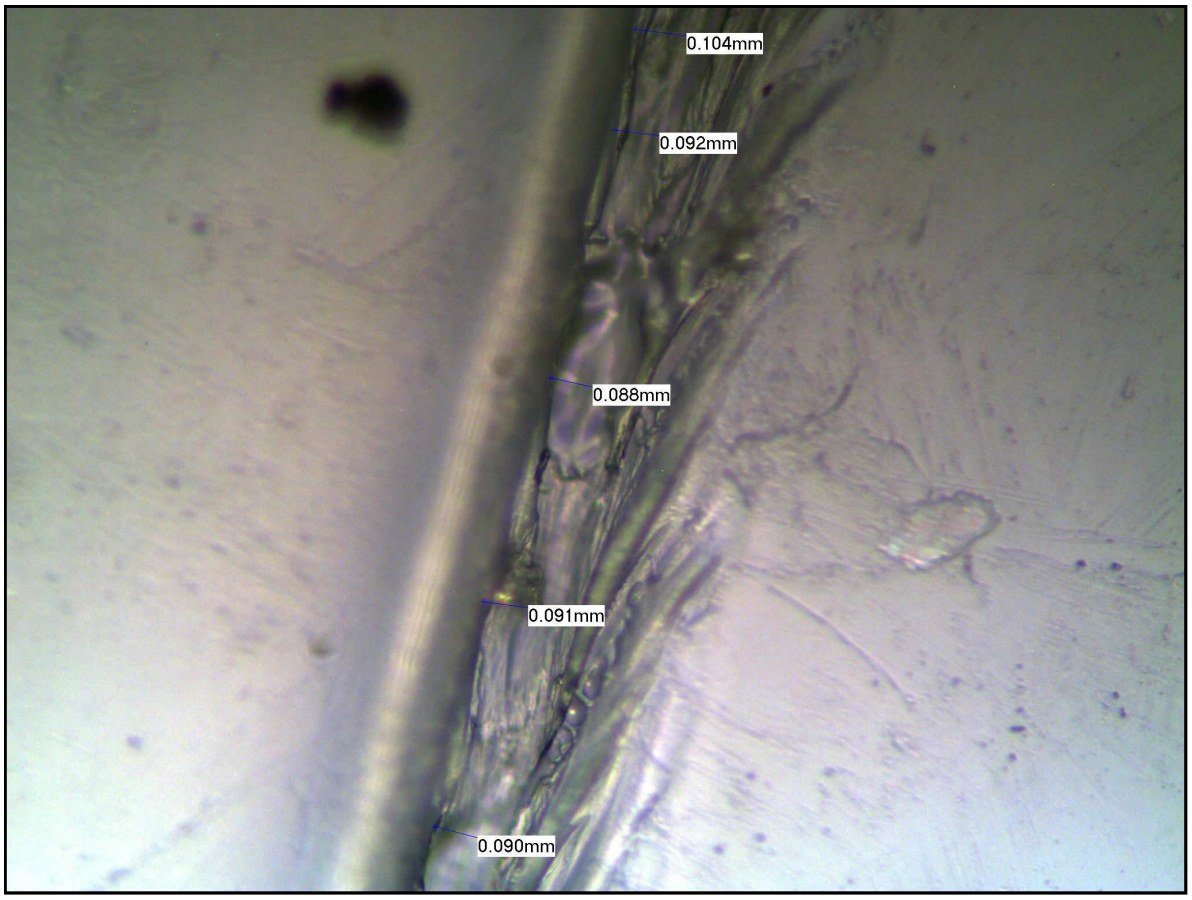

Figure 4.3: Image of striation specimen at 20X magnification

From all three patterns, through optical microscope at a magnification of 20X, it is observed an opaque color formation along the drawn area. Semi crystalline polymers are usually opaque because of light reorientation and being scattered around the crystalline and amorphous regions. The density of such boundaries is lower and thus the transparency is higher either for low (amorphous polymer) or high (crystalline) degree of crystallinity [24]. The opaque optical property is due to crystallization of PVA film when heated blade is used to draw the pattern.

4.3 Differential Scanning Calorimetry

Differential scanning calorimetry is used to measure the percentage of crystallines formed for each specimen. Grid, striation, spot and no pattern (control) have different degree of crystallization based on the pattern complexity. Based on the optical microscope inspection, crystallites occur on the edge of the pattern draw for the entire biomimetics pattern. Since PVA film is translucent, an opaque would be best indication for crystallites formation on the film.

The enthalpy of pure PVA crystal is 138.6 J/g (Hui-Ling Ma *et al*. 2013). Area under the graph of heat flow versus temperature yields the percentage of crystallization. Since PVA film is semi crystalline, the endothermic curve represents crystallization region rather than exothermic region.

The area under the endothermic region is regarded as percentage of crystallization. For grid, the sample were taken at the cross point of biomimetic unit, where the concentration of pattern is at the maximum and it resembles the grid geometry to a certain extend. The specimen for spot shape was taken as a whole one whole unit. For striation sample, two parallel lines of striation were cut to fit into the crucible to retain the striation profile.

Figure 4.4 shows the percentage of crystallization for all biomimetic samples and control sample. PVA grid sample have 49% of crystallization, followed by spot 45%. The percentage of crystallization for striation was 41%. As suspected no pattern sample have the least crystallization of 38%.

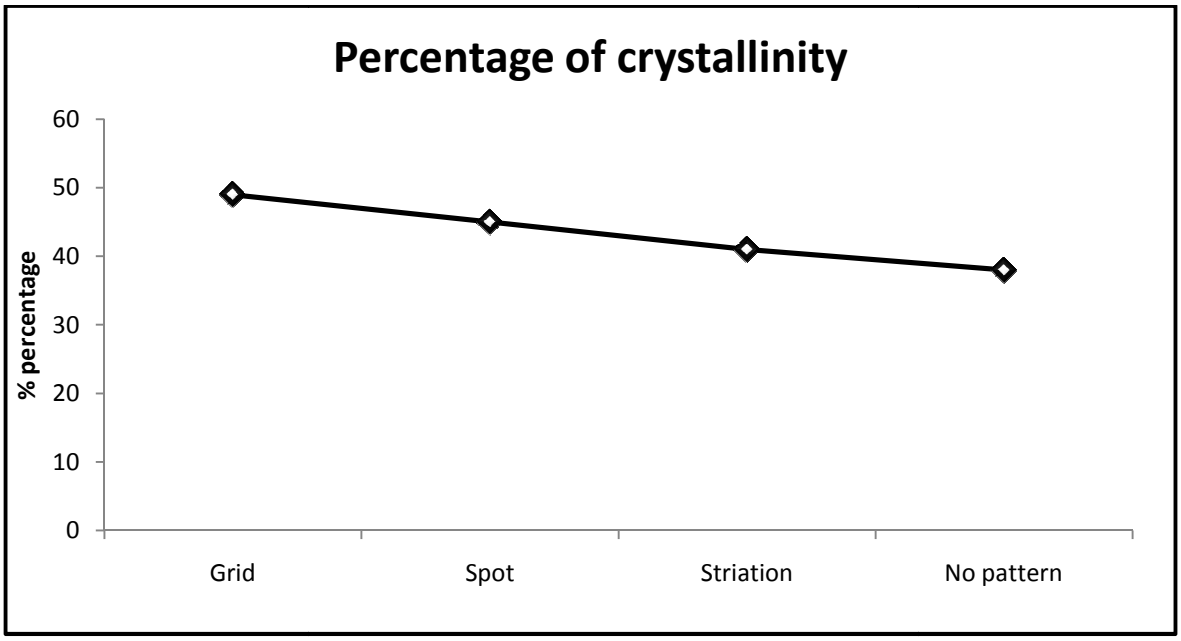

Figure 4.4: Comparison of crystallization for PVA film with biomimetic units

It can be seen that grid posses the highest percentage of crystallinity followed by spot, striation and lastly no pattern (control). The heated geometry blade induce sudden temperature spike in PVA thin film. Crystallization occurs due to chemical reaction at the liquid /solid interface when polymer melts and cools. Grid pattern being highly packed close together leads to highest percentage of crystallites. The grid pattern have more drawn surface when compared to other specimen which in turn having more crystallites.

Spot sample have higher impact then striation sample due to point heating which creates more melt due to higher contact time between heated blade and PVA film surface at a point. Macromolecular crystallization can occur from only the melt or solution state. Striation specimen registered 3rd highest in crystallites. This may be due to the characteristic of striation which has a sparse pattern when compared to spot which is much more compact and with a complete unit and grid which has a higher dense of pattern. No

pattern (control) has certain amount of crystallization due to the nature of PVA thin film as a semi crystalline material. Crystals do form for PVA pure film due to cooling. The percentage of crystallization for each sample is in par with the mechanical properties where crystallization influences the mechanical properties. Table 4.1 shows the crystallization of biomimetic PVA samples and control sample.

Table 4.1: Crystallization of PVA film sample with biomimetic units

Sample	Grid	Spot	Striation	No pattern (control)
% Of crystallization	48.96	44.95	40.82	37.88

4.4 Modulus

Instantaneous modulus was taken during 0% strain and 100% strain. Tangent modulus is the slope of the stress-strain curve at any specified stress or strain. Below the proportional limit the tangent modulus is equivalent to Young's modulus. Above the proportional limit the tangent modulus varies with strain and is most accurately found from test data.

The tangent modulus is useful in describing the behavior of materials that have been stressed beyond the elastic region. When a material is plastically deformed there is no longer a linear relationship between stress and strain as there is for elastic deformations. The tangent modulus quantifies the "softening" of material that generally occurs when it begins to yield.

4.4.1 Striation

Figure 4.5 shows stress versus strain graph for striation shape. Three samples, were tested and result is as below. The graph shows almost accurate result for thin film characteristic until the strain rate is at 100% or 1mm/mm. The 1st sample elongated 2mm more than the 2nd and 3rd sample run. Modulus at initial and 100% strain was calculated using Instron onboard software and discussed in the next section.

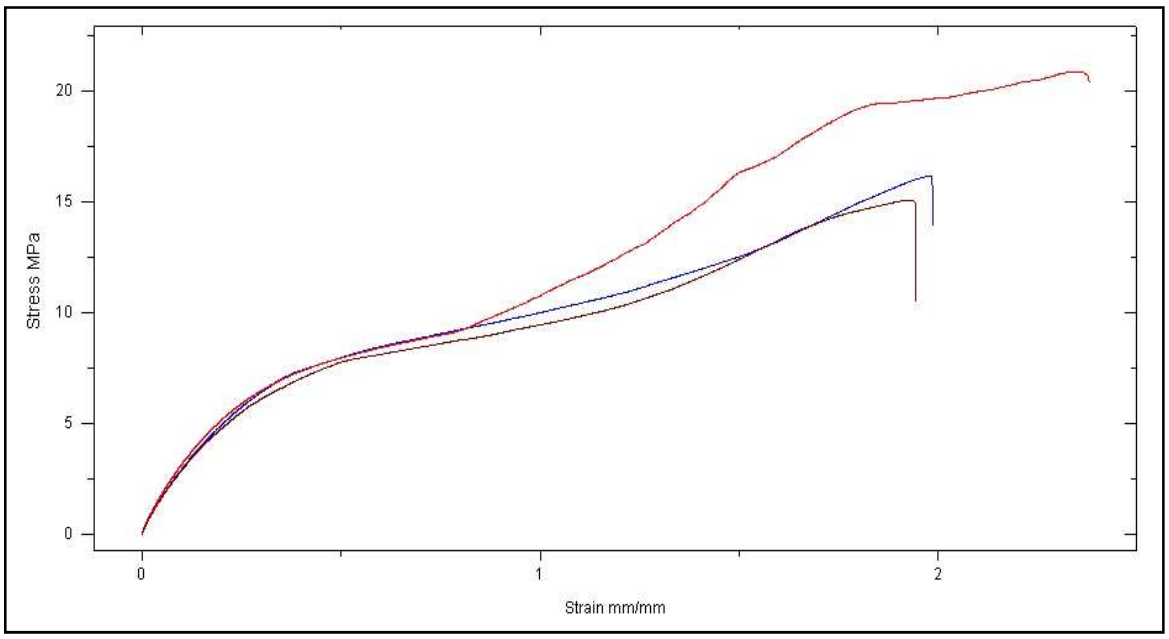

Figure 4.5: Stress versus strain graph for striation sample

4.4.2 Grid

Figure 4.6 show the graph of stress versus strain for grid shape sample. Three samples were tested and the result is as below. The graph shows accurate result up to 150% or 1.5mm/mm of strain for thin film sample. To be noted that, the second sample breaks 1mm short in elongation then other two samples. Modulus at initial and 100% strain was calculated using instron onboard software and discussed in the next section.

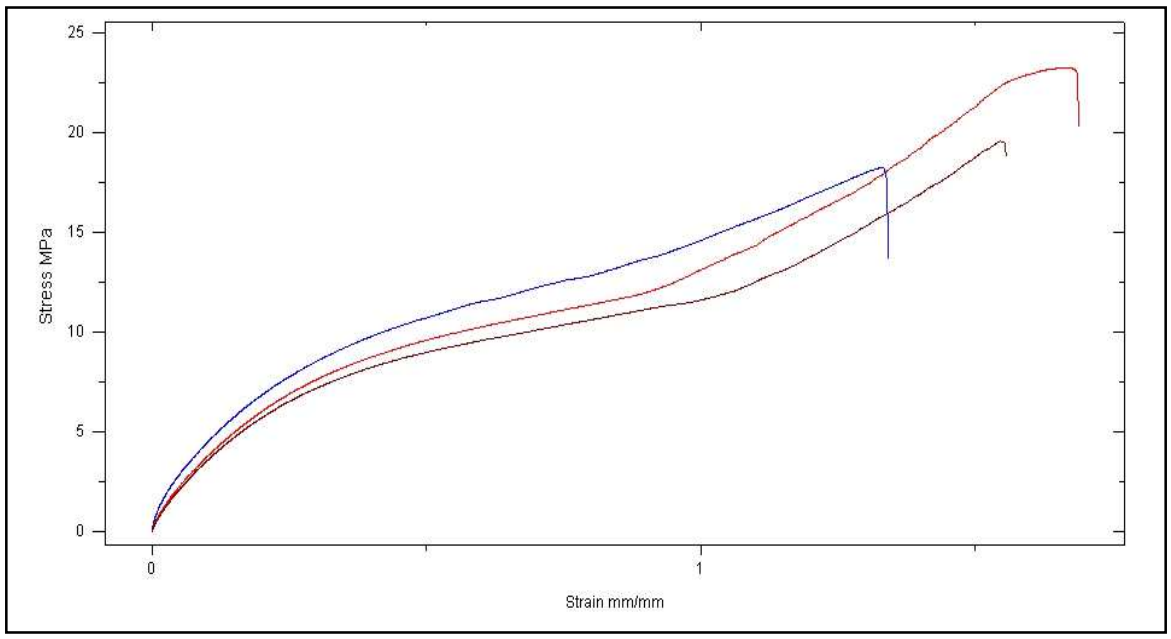

Figure 4.6: Stress versus strain graph for grid shape

4.4.3 Spot

Figure 4.7 shows the graph of stress versus strain graph for spot shape sample. Three samples were tested and the result shown as below. The graph shows accurate result up to 200% or 2mm/mm of strain for thin film sample. All samples breaks at a accuracy of 3mm for each samples.

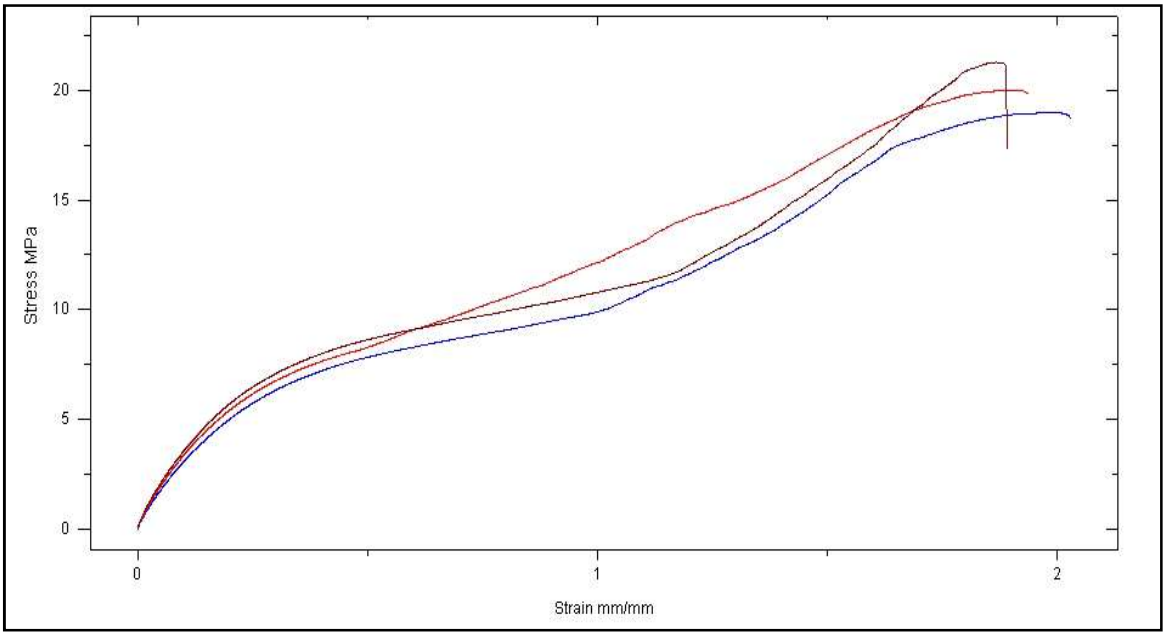

Figure 4.7: Stress versus strain graph for spot sample

4.4.4 No pattern

Figure 4.8 shows the graph of stress versus strain graph for three no pattern samples. The graph shows accurate result up to 200% or 2mm/mm of strain for thin film sample. The first sample had to be forfeit due to oversupply of raw data since the elongation is higher than biomimetics samples.

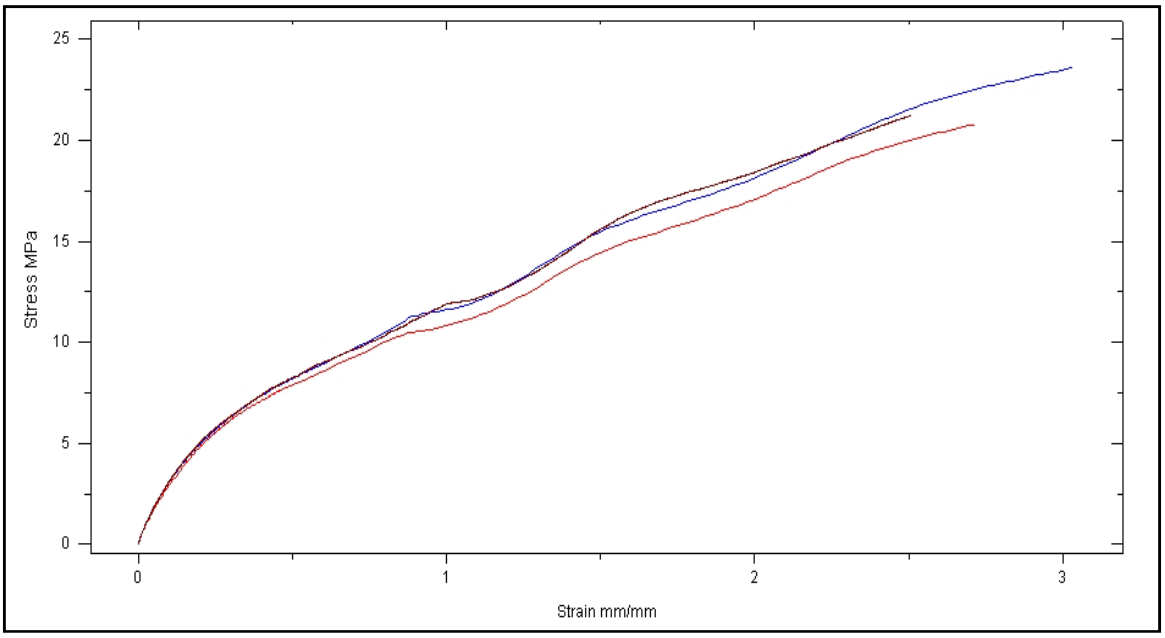

Figure 4.8: Stress versus strain graph for no pattern (control) sample

4.4.5 Comparison of tangent modulus

Three biomimetic unit samples were compared with a no pattern sample. Modulus at initial strain denotes tangent at 0% strain. For no pattern the value is 53.76MPa at the lowest followed by Striation 94.45Mpa, Spot 123.8Mpa and Grid registered the highest value at 242.37Mpa. Figure 4.9 shows the modulus of initial strain with individual unit biomimetic pattern. Table 4.2 shows modulus at initial strain for PVA film sample with biomimetic units compared to no pattern. The error from three samples for grid fluctuates due to randomness of crystal formation when drawing the pattern on the surface of the film.

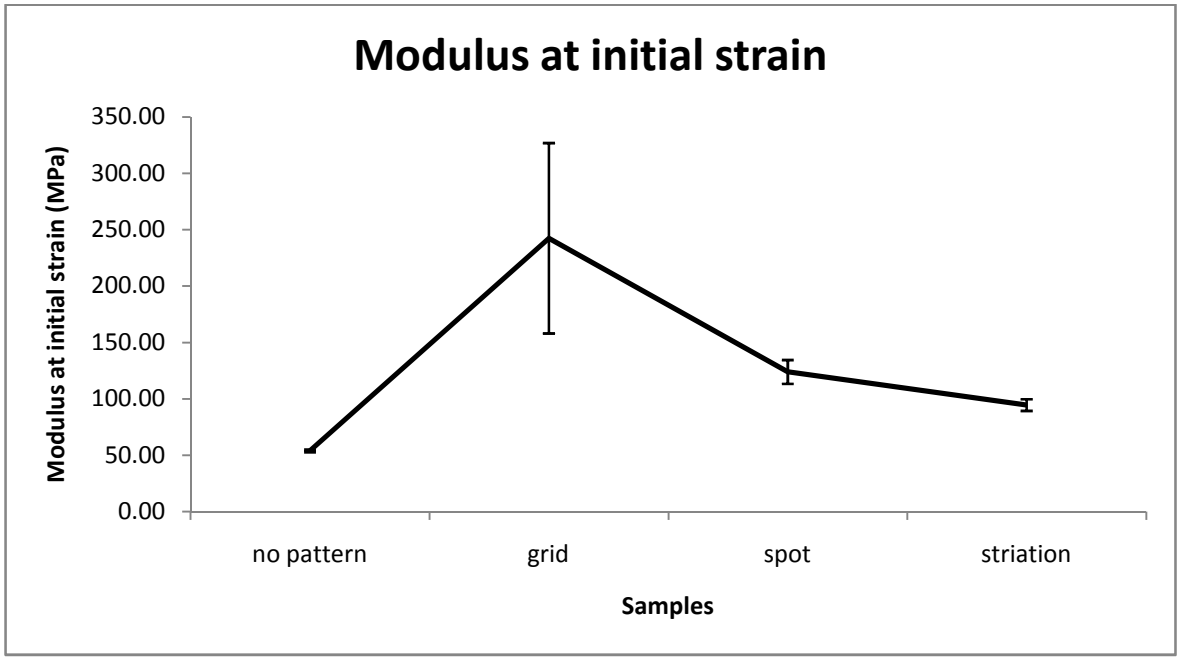

Figure 4.9: Comparison of modulus at initial strain

Table 4.2: Modulus at initial strain for biomimetic units and no pattern

Sample	Grid	Spot	Striation	No pattern
Molus at initial; strain (MPa)	243.37	123.8	94.45	53.76

Figure 4.10 shows the behavior of specimen at 100% modulus. The behavior of the specimen is different for Striation and no pattern specimen where Striation registered the lowest value of 10.66MPa followed by no pattern 11.22MPa, Spot 11.65MPa and the highest modulus at 100% strain was Grid 13.13MPa. However no pattern sample exhibits a better modulus when compare to striation sample. This can be due to the profile of striation sample which is parallel to the axis of elongation. Table 4.3 shows the comparison of modulus at 100% stain for PVA film with biomimetic pattern and no pattern sample.

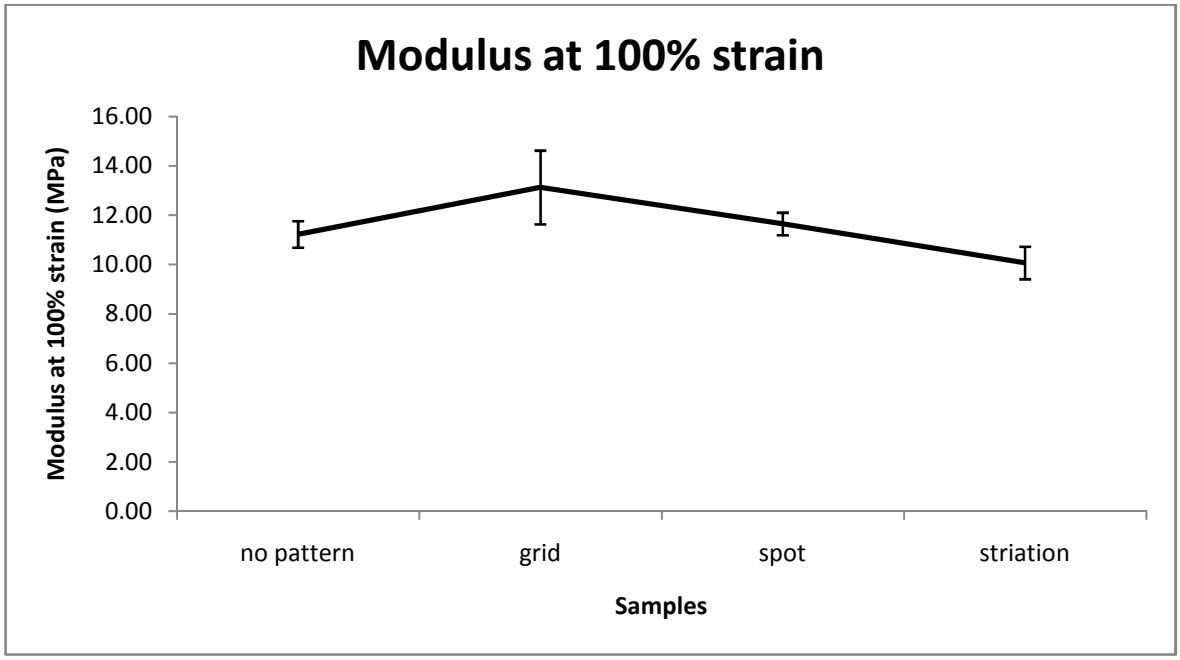

Figure 4.10: Comparison of modulus at 100% strain

Table 4.3: Modulus at 100% strain for PVA film with biomemetic pattern

Sample	Grid	Spot	Striation	No pattern
Modulus at 100% strain (MPa)	13.13	11.65	10.66	12.22

4.5 Maximum elongation

Maximum elongation denotes the total elongation of the specimen before it gives away. Three unique biomimetic units show significant result. Figure 4.11 below shows the comparison between no pattern, grid, spot and striation. As suspected grid marks the lowest percentage of elongation of 151.57% followed by spot 190.90%, striation 208.50% and no pattern registered the maximum elongation of 287.50%. Table 4.4 shows the elongation for PVA thin film with biomimetic pattern and control sample.

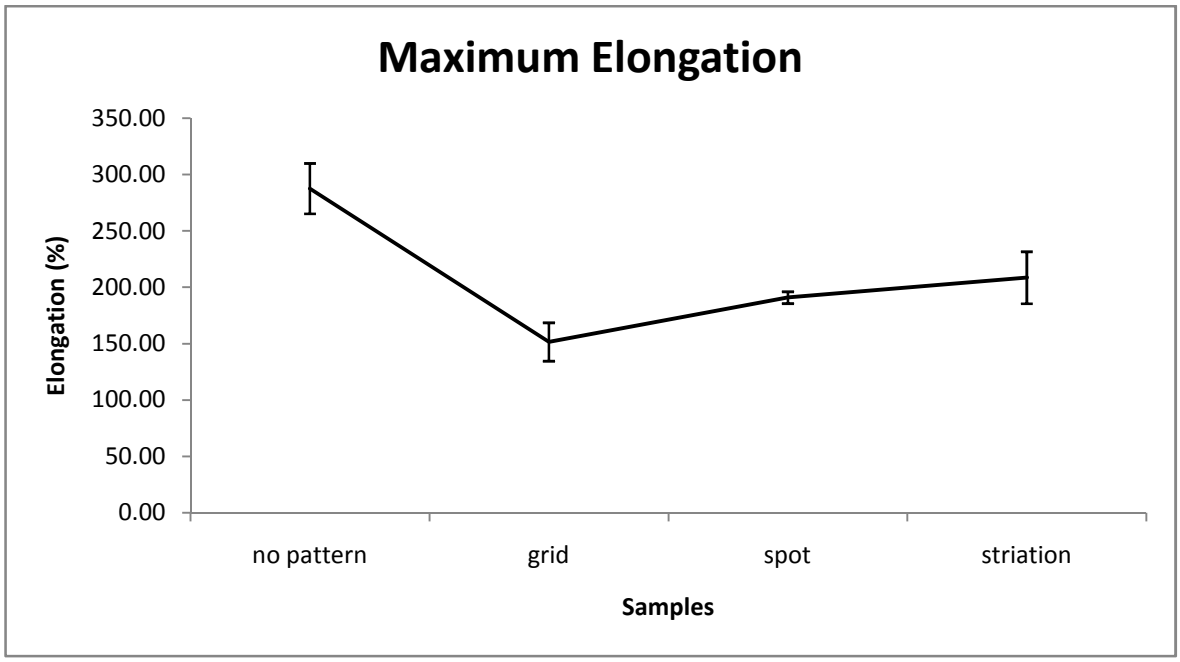

Figure 4.11: Comparison of elongation for biomimetic PVA film and control film

Table 4.4: % of elongation for biomimetic samples

Sample	Grid	Spot	Striation	No pattern
% of elongation	151.57	190.90	208.50	287.50

4.6 Tensile strength

Through universal testing machine, Ultimate Tensile Strength UTS have been calculated for three unique biomimetic shapes. It is the stress at the maximum on the engineering stress–strain curve. This corresponds to the maximum stress that can be sustained by a structure in tension, if this stress is applied and maintained, fracture will result.

Figure 4.12 below illustrates the effect of biommimetic shapes on the PVA thin film specimen. Grid specimen poses the highest value of 20.41MP, followed closely by spot 20.08MPa, striation 17.48MPa and the least was no pattern 14.79MPa.

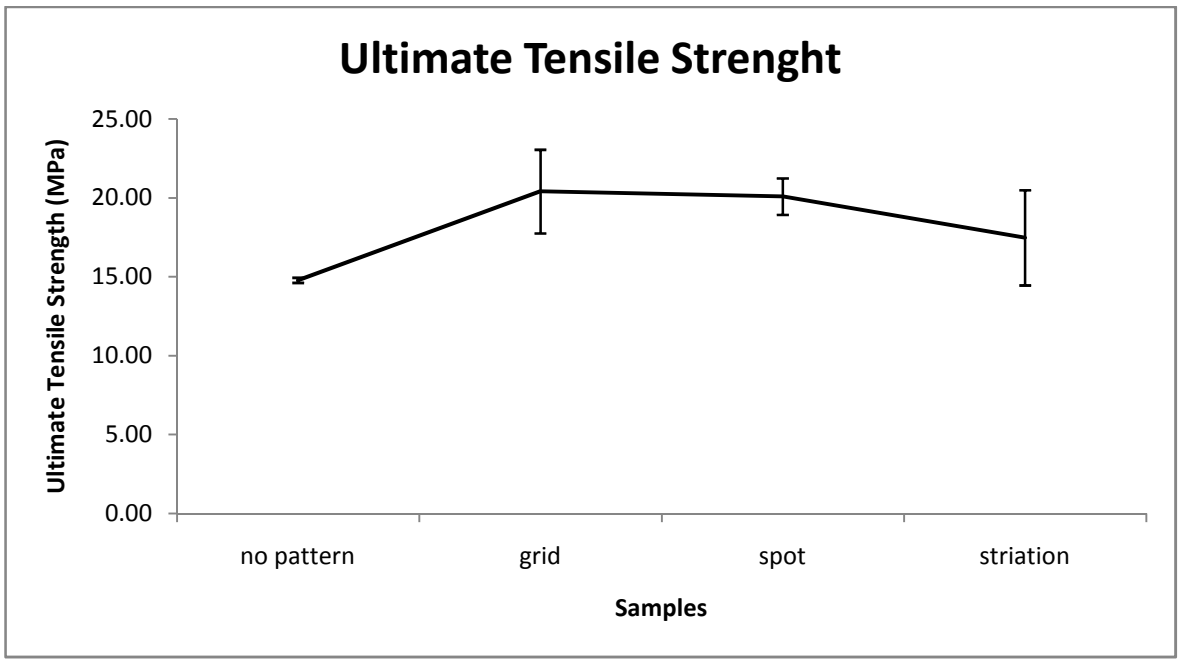

Figure 4.12: Comparison of ultimate tensile strength

Besides UTS breaking strength is that force which is required to break the specimen. Figure 4.13 below shows the comparison between different biomimetic units with no pattern PVA thin film. Again grid pose the highest break strength of 19.33MPa, followed closely by spot 18.56MPa, striation 15.77MPa and the least was no pattern with 14.79MPa.

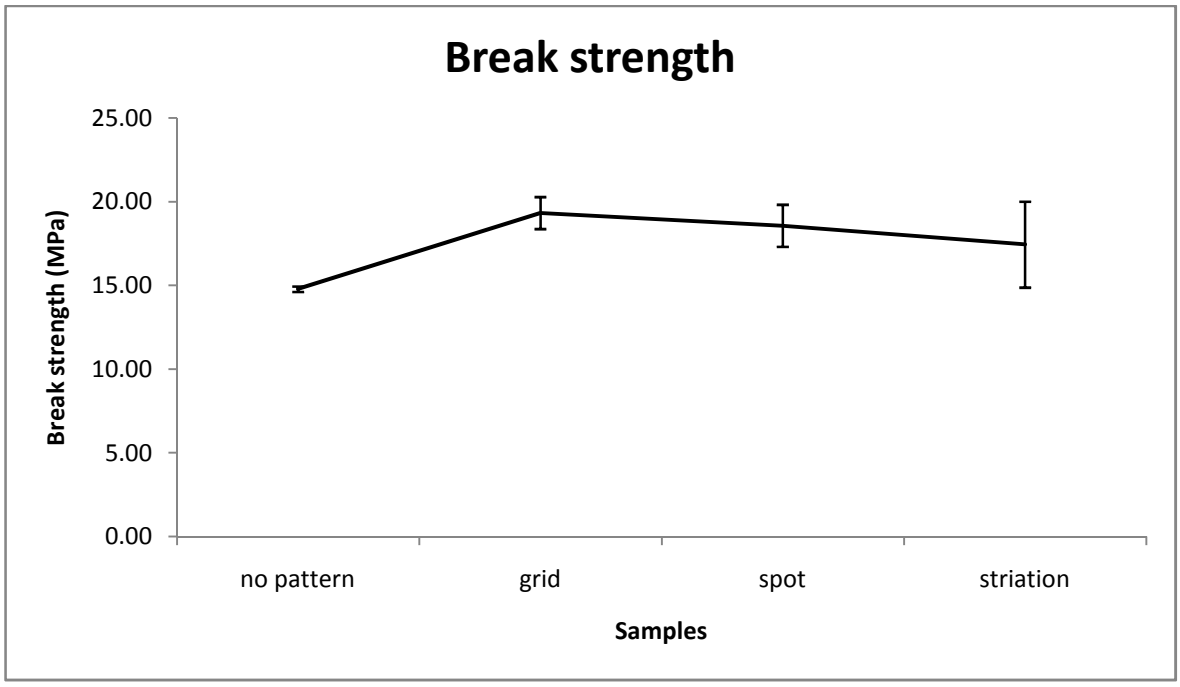

Figure 4.13: Comparison of break strength

4.7 Analysis on Tensile test

Figure 4.14 shows the overall comparison of three unique biomimetic units named grid, spot, striation and no pattern (control) PVA thin films. The mechanical properties in terms of stress versus strain data, were obtained from three repeated tensile tests, and analyzed to determine the average values of the tangent modulus at 0% strain, tangent modulus at 100% strain, break strength and ultimate strength, which are listed in figure below.

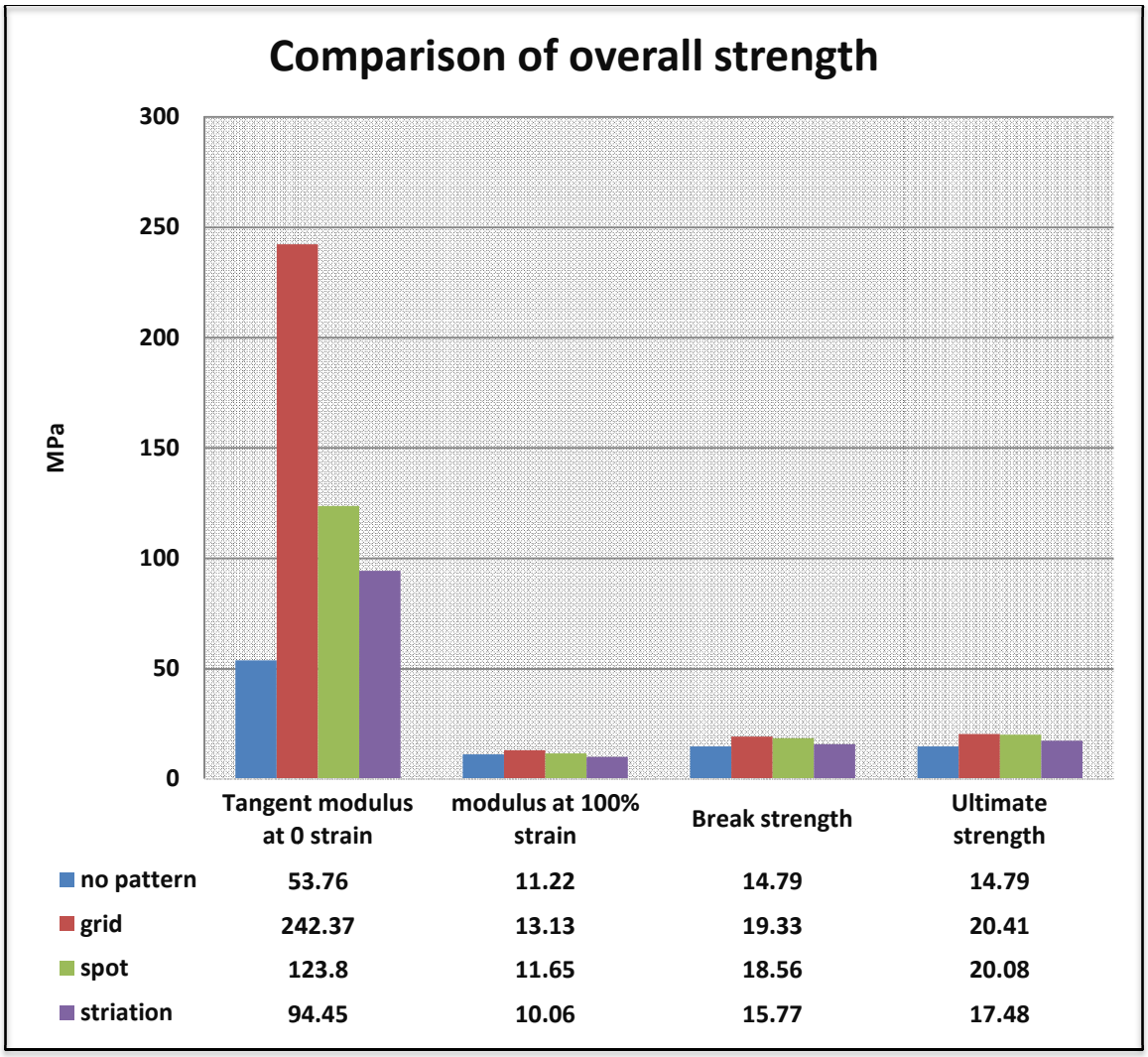

Figure 4.14: Overall comparison for tensile testing for PVA film with biomimetic pattern

It is clearly seen that, biomimetic specimens exhibit more excellent tensile property than no pattern specimen. It can be seen that tangent modulus, tensile strength and ultimate strength, shows that the biomimetic specimens have increased the strength but at a cost of displacement. Tensile property does vary with the shape of the biomimetic unit. Dotted biomimetic specimens display the most marked increase in modulus, tensile strength and break strength but registered the lowest in displacement, while spot and striation biomimetic specimens show a considerable improvement in the modulus, ultimate strength and break strength. By comparison, the overall strength enhancer for the samples was grid units which exhibits the most desirable improvement in tangent modulus break strength and ultimate strength, generating a superior increment relative to the untreated specimen in tangent modulus at 0 strain by 350%, tangent modulus at 100% strain by 17%, break strength by 31% and ultimate strength by 40% with a decrease in maximum displacement by 47%.

The microstructure characteristics after the biomimetic units were drawn using heated blade have a beneficial influence on improving mechanical properties, such as tensile strength. From the result of optical microscope all three specimen poses crystallites to a certain degree based on the pattern. The introduction of crystals in PVA thin film does affect the mechanical properties. This can be judged based on grid specimen that has higher tangent modulus, and strength when compared to striation, spot and no pattern. The percentage of crystallization in grid specimen was the highest as reported in DSC analysis.

The crystalline region essentially serves as an extra crosslink to distribute stress acting on the PVA thin film. Strong intermolecular forces in semi crystalline PVA film prevent softening of the specimen even above the glass transition temperature. The elastic modulus of polymers changes significantly only at high melting temperature (Georg

Menges *et al*, 2002).The percentage of crystallization affects drastically the mechanical properties of a material. Higher crystallinity results in a harder, stiffer and more thermally stable but in a exchange, it will be less ductile. This can be observed by grid specimen having the least displacement of 81.23mm compared to no pattern specimen which has 153.2mm of maximum displacement. Semi crystalline polymers also have a strong anisotropy of their mechanical properties along the direction and perpendicular to the molecular arrangement (Martin Bonnet. 2008)

The biomimetic pattern does influence the mechanical properties with the introduction of crystallites in the thin film as no pattern specimen registered the lowest value in modulus, tensile strength. This is due to PVA films are mostly amorphous when it is being casted. Crystallization will only starts on the final drying stages and proceeds slowly, influenced by the ambient humidity. If the ambient humidity is low, the drying specimen becomes glassy, and crystal growth becomes arrested before extended crystallites can develop and impinge (K. E. Strawhecker *et al*, 2001). PVA is an atactic material but since hydroxyl groups are small enough. Crystallizations do occur and fit into the lattice without disrupting it. Unlike in the case of other atactic polymers such as rubber and silicon which don’t tend to crystallize (G. W. Ehrenstein *et al*, 2001).

4.8 Dynamic mechanical analysis result

The behavior of thin film PVA with unique three biomimetic pattern was analyzed with variable frequency from 10Hz to 270Hz. Loss modulus and Storage modulus were taken from each sample named striation, grid and spot. Those patterns were compared to the no pattern PVA thin film.

4.8.1 Loss Modulus

Figure 4.15 below illustrates the effect of variable frequency from 10Hz to 270Hz for Loss Modulus. All sample increases linearly up to 80Hz identically all samples begin to have a smaller slopes up to 270Hz. Grid and striation have almost same loss modulus until 50Hz. Significant difference can be noticed after 60Hz up to 270Hz. The slopes of the spot sample also deteriorate after 130Hz where the difference between striation and spot are almost identical if compared to initial comparison with grid.

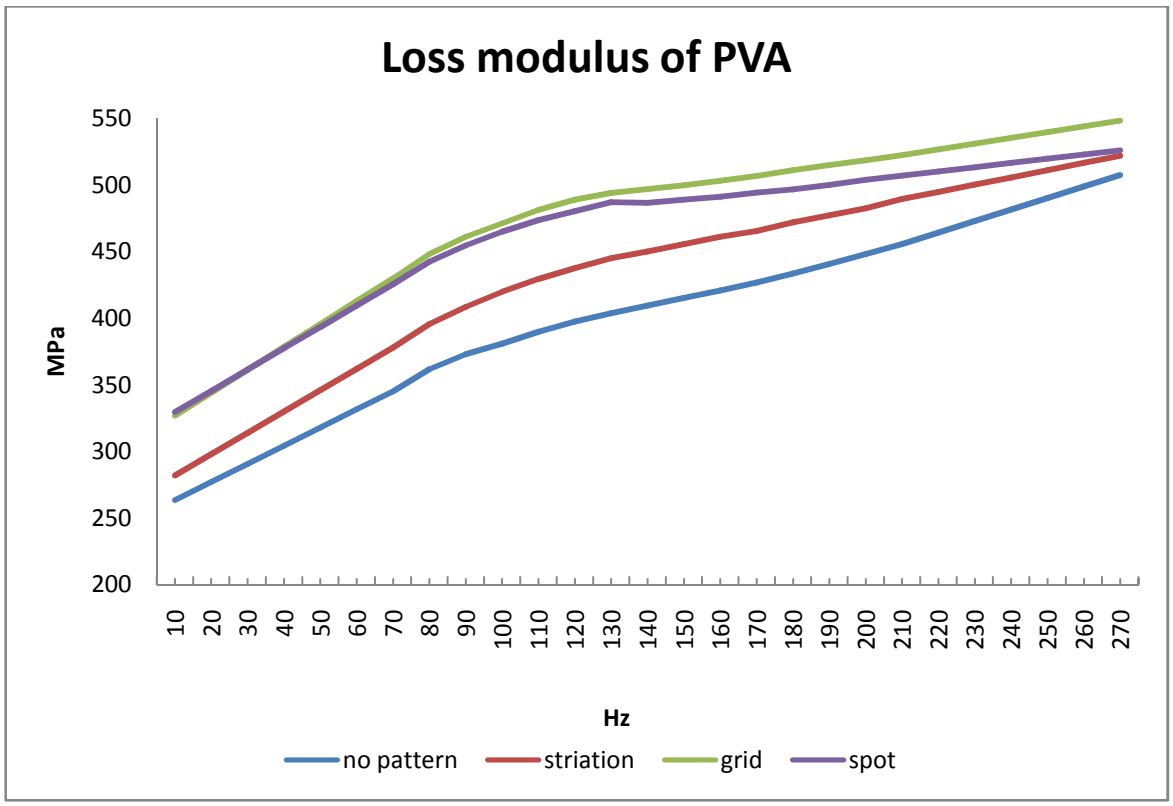

Figure 4.15: Comparison of loss modulus

4.8.2 Storage Modulus

Figure 4.16 below shows the effect of variable frequency from 10Hz to 270Hz applied to the PVA thin film with three unique biomimetic patterns and compared to the un patterned sample. All four patterns show a linear increment up to 90Hz. To be noted, grid and spot specimen have registered almost identical difference in Storage Modulus across the frequency sweep. For striation and no pattern, the storage modulus was almost identical for a frequency less than 30Hz. beyond 30Hz striation have steeper slope.

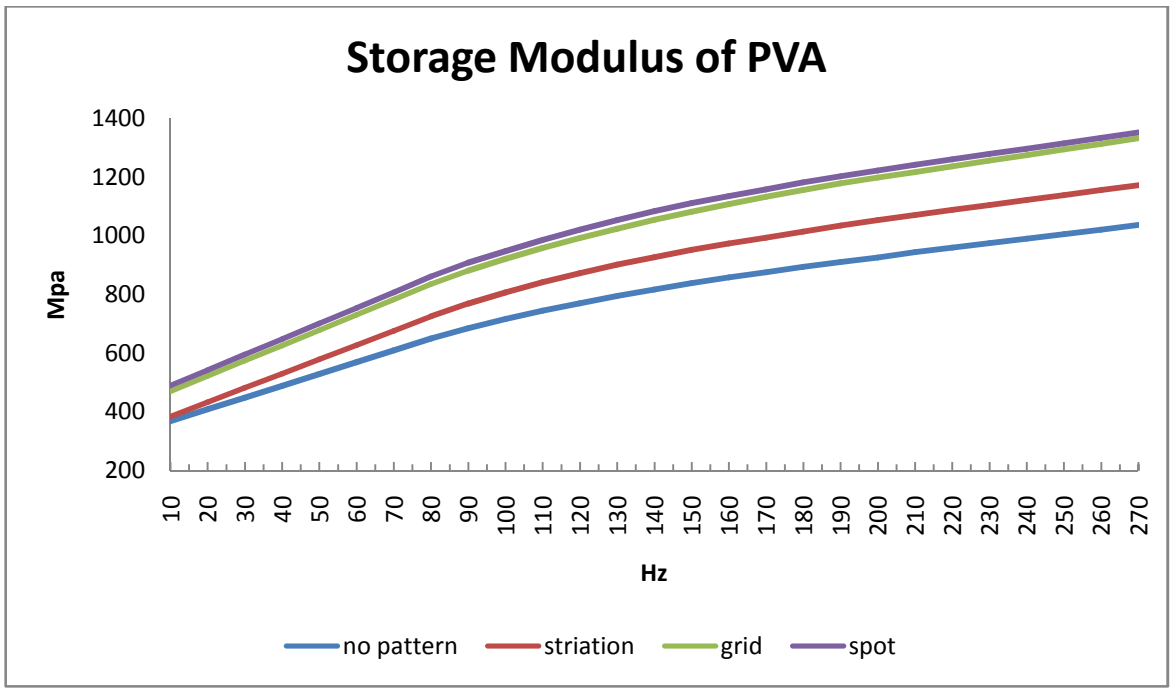

Figure 4.16: Comparison of storage modulus

4.8.3 Analysis on DMA

From the graph of storage modulus it can be seen that all the specimen values are higher than the corresponding value for loss modulus over the entire frequency range from 10Hz to 270Hz. This result shows that thin film PVA with and without biomimetic pattern exhibit more elastic behavior than viscous counterpart Marco (Cespi *et al*, 2011). Loss modulus and storage modulus for all the specimen increases linearly up to 80-90Hz and the increment become slow beyond 90Hz until 270Hz.

The frequency dependence of storage modulus and loss modulus suggests that these thin films PVA have amorphous consistency than glassy (Shi,A. *et al*, 2012). However, the introduction of grid pattern on the specimen results into the increase in storage modulus and loss modulus simultaneously. This suggests that both elastic and viscous properties were

enhanced due to the amorphous nature of PVA and crystallization of the specimen due to pattern.

For all three biomimetic unit specimens, loss and storage modulus were enhanced when compared to the no pattern (control) specimen, it exhibits viscoelasticity properties. A viscoelastic material converts mechanical energy into to heat by internal friction. The polymer structure looks like a clump of spaghetti and as the material is deflected, these polymer chains rub together generating friction and heat (Bryan C *et al*). From DSC analysis and optical image analysis, crystallization plays a major part in enhancing both viscous property and elastic property to certain extend.

However the linear increment in when the frequency increases from 10Hz to 270Hz suggest that friction plays a role in generating heat as the crystallites brittle chain rub together to generate heat thus creating friction. Increasing frequency leads to greater defection. It can be proven since no pattern sample has lowest loss modulus value for the entire frequency range and in contrast, grid specimen having the highest loss modulus value.

Since the strain displacement of 10µm is on the elastic region for PVA thin film sample. The introduction of biomimetic pattern increases the elastic property of the PVA thin film. From the graph of storage modulus, the difference between no pattern sample and striation sample increase when the frequency increases. The introduction of pattern promotes to the growth crystals, when the frequency increases, the strong bonding between crystallites holds together to promote more elastic condition than amorphous region.

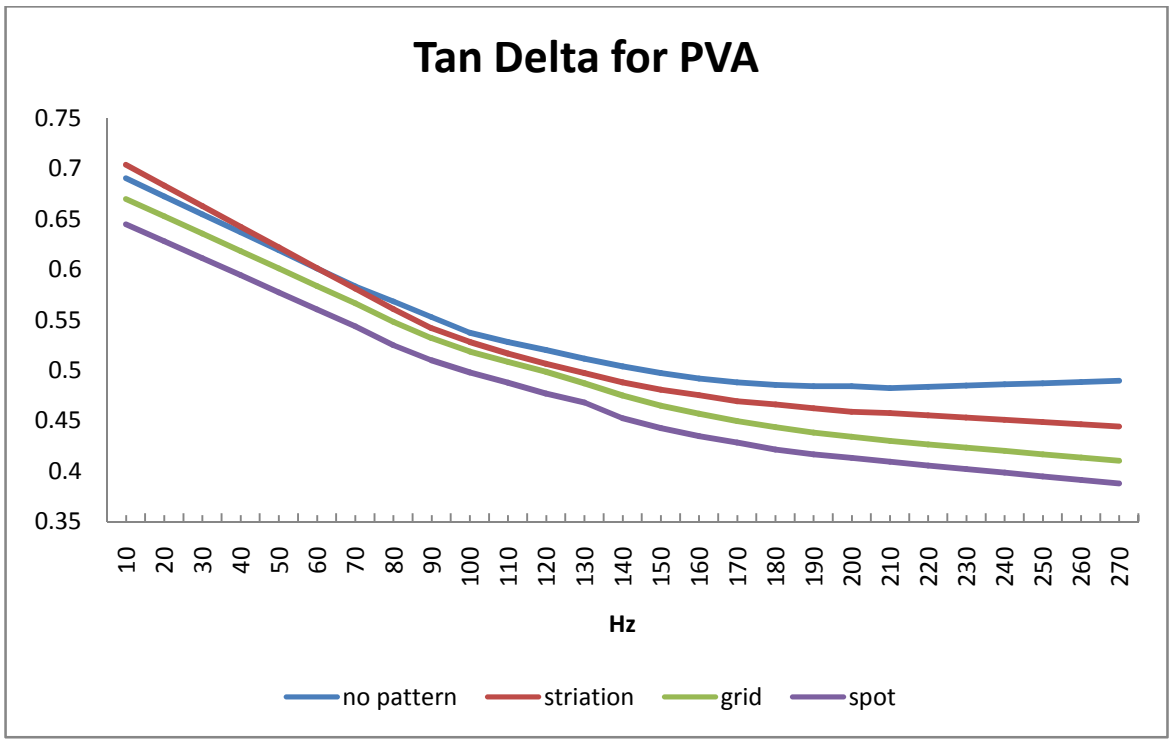

Figure 4.17: Comparison of damping factor

Figure 4.17 above shows tan δ. Damping factor for all three specimen compared to no pattern sample (control). Striation specimen has the highest value until the frequency range of 60Hz. Above 60Hz no pattern registered a higher tan δ than all three biomimetic component. For purely elastic material, the phase angle δ=0 , where else for purely viscous material the phase angle is 90°. The increase in tan δ suggest that the viscous component is affected to a greater extent than the elastic component where it does suggest that viscous component due to lower crystallites in no pattern sample. But since striation has a better viscous property below 60Hz, this can be due to the pattern profile which has two parallel lines to the displacement acting. Same goes to grid pattern which registered the second lowest value (more elastic property than viscous) than spot pattern.

CHAPTER 5

CONCLUSION

5.1 Conclusion

In this research project, the main aim was to enhance the mechanical properties for thin film PVA for the application of MAVs wing membrane material. Three biomimetic shapes named grid as a pattern found in dragonfly and butterfly wings, spot shape that can be found on ground beetle and striation shape as tree leaf were mimicked into PVA thin film by drawing the pattern using heated geometry blade. These biomimetic structures have been evolved through centuries to adapt the living scenarios. Researchers have successfully mimic those patterns into metallic material, results shows an increment in mechanical properties with enhanced ductility. However this research was intended to mimic those patterns into polymer for the application of MAVs wing membrane.

Four pure PVA thin films named grid, striation, spot and no pattern (control) with 3 specimens each examined for any mechanical properties enhancement. The result for this research project is summarized as below:

a) Based on the physical appearance using optical microscope at 20X magnification. All three biomimetic specimen exhibits enhanced crystallinities. Crystal formation can be seen as opaque appearance along the grid pattern. For spot units, hardened PVA film surface be seen on the outer radius of the spot diameter. Striation shape also exhibits opaque appearance along the pattern lines. These crystallization is due to a sudden intense heating and cooling from the geometry blade tip that was used to draw the unique biomimetic pattern.

b) Further to the investigation of the percentage of crystallization due to biomimetioc patten was relieved through differential scanning calorimetric tester. Four samples grid, striation, spot and no pattern (control) were tested on a temperature range of 30°C to 300°C with 10°C increment every minute. As suspected, result shows that grid specimen had a highest percentage of crystallinity, followed by spot, striation and the least no pattern (control). This is due to the density of pattern where grid posses more complex pattern and spot have a concentrated crystals. However, PVA is not a complete amorphous polymer. This can be verified by no pattern sample where pure PVA film as it is being tested and resulting 38% of crystallization.

c) Mechanical testing was performed using Instron universal testing machine with 100N load cell. Results shows grid pattern enhance drastically on tangent modulus (stiffer properties) and enhanced tensile strength and break strength. This followed by spot and striation. The strength enhancement is associated with crystallization of the biomimetic pattern. Unlike metallic material, the biomimetic pattern gives negative effects to the ductility of polymer material.

Since the thickness of the film is less than 1mm and the introduction of the biomimetic pattern further reduces the thickness relatively. Stress distribution is not evenly distributed when PVA film is being pulled, the weak point where the pattern carved in the already thin PVA film makes vulnerable to stress introduction. PVA films with biomimetic pattern don't exhibit a good displacement behavior when compared to no pattern (control).

d) Viscoelastic behaviors over a frequency range of 10Hz to 270Hz were analyzed amongst grid, spot, striation and no pattern (control). All samples gains increment in loss modulus when the frequency increases. Samples with biomimetic pattern have higher loss modulus across the frequency range with grid poses the highest loss modulus and no pattern specimen having the lowest value. The heat generated through the friction of crystallites lead to loss modulus spike for the biomimetic specimens. Storage modulus was measured to analyze the degree of elasticity. The introduction of biomimetic pattern increases the elastic property of the PVA thin film, since the displacement in DMA is low 1µm which is lower the elastic limit, the strong bonding between crystallites holds together to promote more elastic condition than amorphous region. Damping factor was calculated through the ratio of loss and storage modulus. Striation specimen has the highest value until the frequency range of 60Hz. For purely elastic material, the phase angle $\delta=0$, where else for purely viscous material the phase angle is 90°. The increase in tan δ suggest that the viscous component is affected to a greater extent than the elastic component where it does suggest that viscous component due to lower crystallites in no pattern sample. But since striation has a better viscous property below 60Hz,

this can be due to the pattern profile which has two parallel lines to the displacement acting. Same goes to grid pattern which registered the second lowest value (more elastic property than viscous) than spot pattern.

5.2 Recommendation and further studies

There is still plenty of room for the improvement of thin films for Micro Aerial Vehicle MAV wings membrane. Biomimetic structure does promise an extension of mechanical properties in terms of stiffness and strength. Ductility can also be improved if the thickness of the pattern revamped. The areas for improvement that can be further explored are;

a) Vibration analysis of wing membrane, the introduction of pattern on the surface of the film leads to different resonance frequency. To localize the resonance frequency, i.e. concentrated pattern to be drawn in a specific surface of the film rather than symmetry.
b) The influence of variable temperature on drawing the biomimetic pattern using geometry cutter. The temperature will influence the crystallites formation and thus the ideal temperature is unknown for PVA thin film.
c) Pure PVA is water soluble, thus it is not an ideal for outdoor MAVs, an addition of crosslink to the polymer chain to promote water resistant PVA film should be studied by researcher.

BIBLIOGRAPHY

Karl R. Klingebiel. (2006) *Computational aerodynamics of flapping flight using an indicial response method*.Department of Aerospace Engineering. The Pennsylvania State University

Newcome, L. R. (2004*) Unmanned Aviation - A Brief History of Unmanned Aerial Vehicles*. AIAA, Reston, VA.

C.thipyopas, A.B sun, C.bernard J.H Moschette. (2011) Application of electro active materials to a coaxial rotor NAV. *Proceedings of the International Micro Air Vehicles conference 2011 summer edition.*

C. Thipyopas, N. Intaratep. (2011) Aerodynamics Study of Fixed-Wing MAV: Wind Tunnel and Flight Test. *Proceedings of the International Micro Air Vehicles conference 2011 summer edition.*

T. Nick Pornsin-sirirak, Y.C. Tai, H. Nassef, C.M. Ho. (2001) Titanium-alloy MEMS wing technology for a micro aerial vehicle application *Sensors and Actuators A* 89 95-103.

H. Rajabi, M. Moghadami, A. Darvizeh. (2011) Investigation of Microstructure, Natural Frequencies and Vibration Modes of Dragonfly Wing. *Journal of Bionic Engineering* 8 165–173.

Jiyu Sun, Bharat Bhushan C. R. (2012) The structure and mechanical properties of dragonfly wings and their role on flyability Jiyu Sun , Bharat Bhushan C. R. *Mecanique* 340 3–17

S.K.Saxena. (2004) *Polyvinyl alcohol (PVA)* Chemical and Technical Assessment (CTA) First draft. FAO

Ulrich Siemann (2005) Solvent cast technology – a versatile tool for thin film production.*progress in colloid and polymer science* 130: 1–14 DOI 10.1007/b107336

Hong Zhou, Na Sun , Hongyu Shan , Dianyi Ma , Xin Tong , Luquan Renb. (2007) Bio inspired wearable characteristic surface: Wear behavior of cast iron with biomimetic units processed by laser. *Applied Surface Science* 253 9513–9520

Chuanwei Wang, HongZhou, ZhihuiZhang, YuZhao, DalongCong, ChaoMeng Peng Zhang,LuquanRen. (2013) Mechanical property of low carbon steel with biomimetic units in different shapes. *Optics & Laser Technology* 47 (2013) 114120.

Halyk R M, Hurlbut L M. (1968) Tensile and shear strength characteristics of alfalfa stems. *Transactions of American Society of Agricultural Engineering*, 1968,11, 256–27.

Zebrowski J.(1999) Dynamic behaviour of inflorescence-bearingTriticale and Triticum stems *Planta*, 1999,207, 410–417.

Wegst U G K, Ashby M F.(2004) The mechanical efficiency of natural materials. *Philosophical Magazine*, 2004, 84, 2167– 2181

Peng X H, Fan J H, Chen B. (2000) Microstructure of natural biocomposites and research of biomimetic composites. *Acta Materiae Compositae Sinica*, 2000, 17, 59–62.

J.G. Needham, A genealogic study of dragon-fly wing venation, *Proc. U.S. Natn. Mus*. 26 (1903) 703–764.

M. Kempf (2000) Biological materials, determination of Young's moduli of the insect cuticle (dragonflies, 2000; *Anisoptera*), Application note, Hysitron Inc,www.hysitron.com

Zhihui Zhang, Luquan Ren, Hong Zhou, Zhiwu Han, Xin Tong, Yu Zhao, Li Chen. (2010) Effect of Thermal Fatigue Loading on Tensile Behavior of H13 Die Steel with Biomimetic *Surface Journal of Bionic Engineering* 7 (2010) 390–396

Chuanwei Wang , Hong Zhou, Zhihui Zhang, Yu Zhao, Peng Zhang, Dalong Cong, Chao Meng, Fuxing Tan. (2012). Tensile property of a hot work tool steel prepared by biomimetic coupled laser remelting process with different laser input energies. *Applied Surface Science* 258 (2012) 8732– 8738

Annual book of ASTM standards section 8, *volume 8.01 Plastic* 1: D 253 – D2343

Kevin Menard. (2008). Dynamic Mechanical Analysis: A Practical Introduction, *2nd Edition, CRC Press.*

Montgomery Shaw, William J. Mac Knight. (2005). *Introduction to Polymer Viscoelasticity, Wiley,* New York, 2005.

Hui-Ling Ma, Youwei Zhang, Qi-Hui Hu, Shunlun He, Xiaofeng Li, Maolin Zhai, Zhong-Zhen Yu.(2013) Enhanced mechanical properties of poly(vinyl alcohol) nanocomposites with glucose-reduced graphene oxide. *Materials Letters*

Georg Menges, Edmund Haberstroh, Walter Michaeli, Ernst Schmachtenberg. (2002) *Plastics Materials Science.* Hanser Verlag, 2002, ISBN 3-446-21257-4

Martin Bonnet. (2008) *Plastics in engineering applications: properties, processing and practical use of polymeric materials.* (in German) Vieweg+Teubner Verlag, 2008 ISBN 3-8348-0349-9.

K. E. Strawhecker, E. Manias. (2001) *AFM of Poly(vinyl alcohol) Crystals Next to an Inorganic Surface*. Macromolecules 2001,34,8475-8482.

G. W. Ehrenstein, Richard P. Theriault (2001). *Polymeric materials: structure, properties, applications*. Hanser Verlag. pp. 67–78. ISBN 1-56990-310-7.

Marco Cespi, Giulia Bonacucina, Giovanna Mencarelli, Luca Casettari, Giovanni Filippo Palmieri. (2011). Dynamic mechanical thermal analysis of hypromellose 2910 free films. *European Journal of Pharmaceutics and Biopharmaceutics*. 79 (2011) 458–463

Shi,A. et al. (2012) Characterization of starch film containing starch nanoparticles. Part2: Viscoelasticity and creep properties. *Carbohydrate Polymers.* 89, 269-274

Bryan Crawford, Erik Herbert, Harold Herzlich. *Measuring the gradient of storage and loss modulus on elastomer compounds*. Analytical service, Nanomechanics, Inc.

APPENDIXES

A1. Result data for tangent modulus at 0% strain for all 3 specimens for the biomimetic PVA thin film. All value in MPa.

Sample	1	2	3	Average	Std Dev
no pattern	54.54	52.97		53.76	1.110157646
grid	174	336.7	216.4	242.37	84.40096761
spot	112.8	124.8	133.8	123.80	10.53565375
striation	91.49	100.5	91.36	94.45	5.239856868

A2. Result data for tangent modulus at 100% strain for all 3 specimens for the biomimetic PVA thin film. All value in MPa.

Sample	1	2	3	Average	Std Dev
no pattern	10.84	11.6		11.22	0.537401154
grid	11.63	14.62	13.13	13.13	1.495002787
spot	11.56	12.14	11.24	11.65	0.456216323
striation	10.75	9.996	9.444	10.06	0.655598454

A3. Result data maximum elongation for all 3 specimens for the biomimetic PVA thin film. All value in mm.

Sample	1	2	3	Average	Std Dev
no pattern	271.7	303.3		287.50	22.34457429
grid	154.6	133.2	166.9	151.57	17.05354313
spot	196.8	189.2	186.7	190.90	5.260228132
striation	235	198	192.5	208.50	23.11384866

A4. Result data break strength for all 3 specimens for the biomimetic PVA thin film. All value in MPa.

Samples	1	2	3	Average	Std Dev
no pattern	14.9	14.67		14.79	0.16263456
grid	19.58	18.27	20.13	19.33	0.955527777
spot	18.66	19.77	17.26	18.56	1.257789066
striation	20.34	16.5	15.48	17.44	2.562732916

A5. Result data for ultimate tensile strength for all 3 specimens for the biomimetic PVA thin film. All value in MPa.

Samples	1	2	3	Average	Std Dev
no pattern	14.9	14.67		14.79	0.16263456
grid	19.58	18.27	23.37	20.41	2.64859082
spot	18.97	19.99	21.28	20.08	1.157626883
striation	20.86	16.5	15.07	17.48	3.016029399

A6. Graph of heat flow against temperature for DSC analysis using grid specimen.

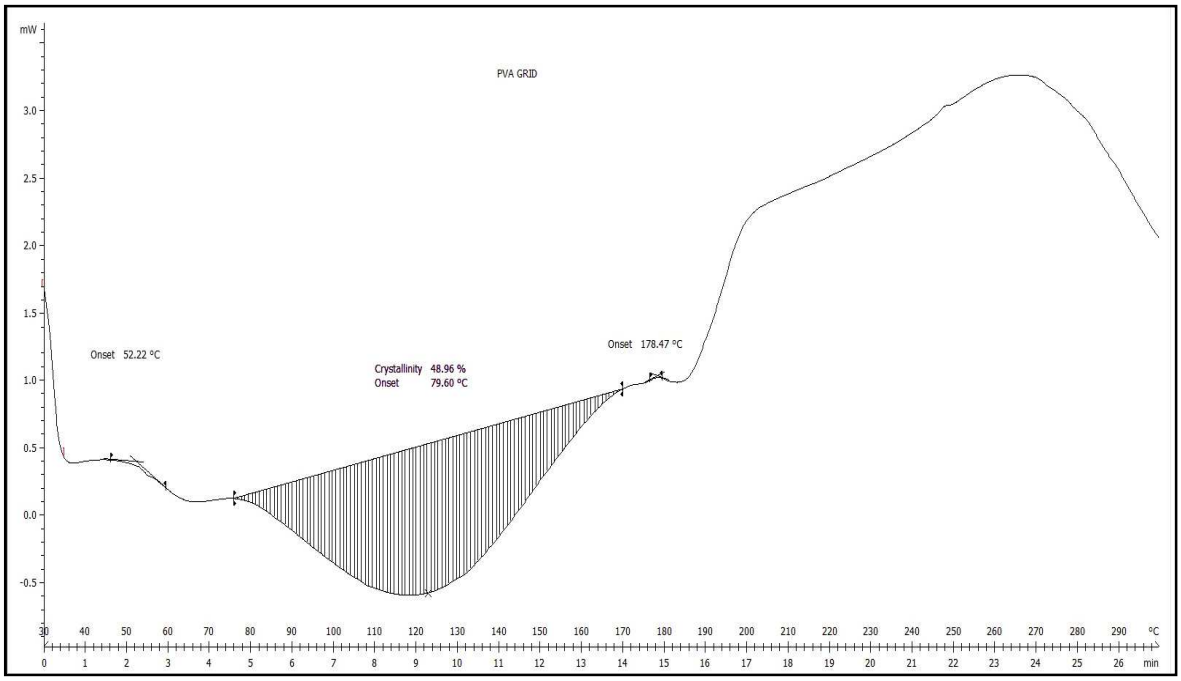

A7. Graph of heat flow against temperature for DSC analysis using striation specimen.

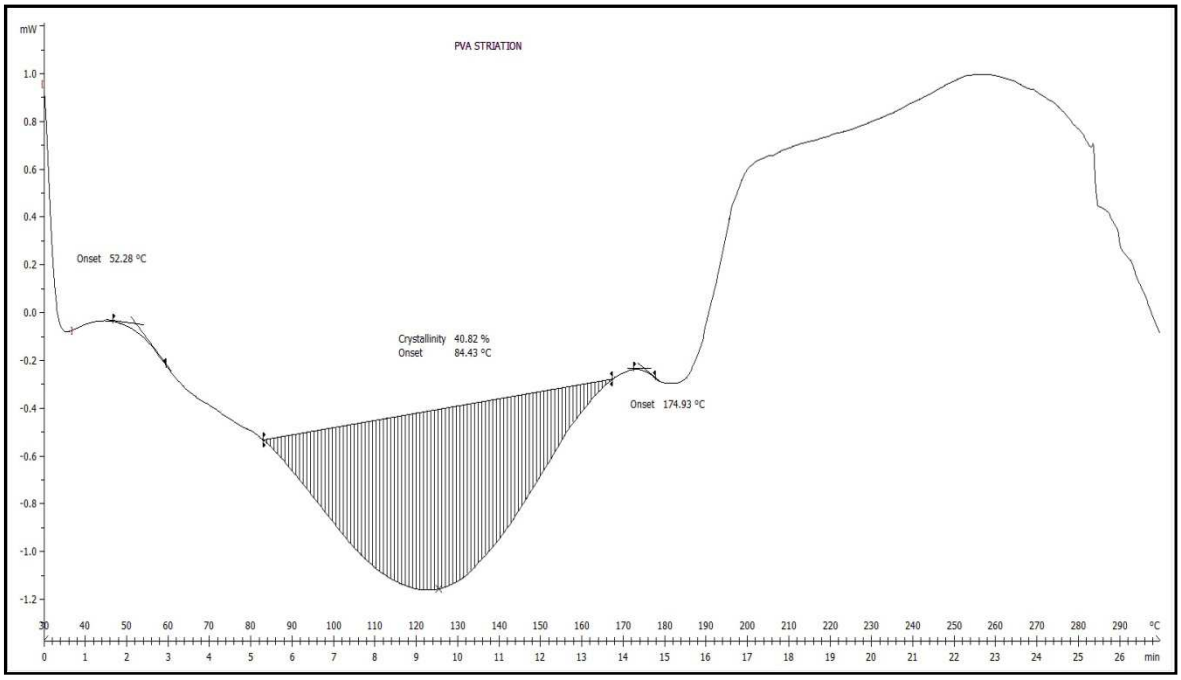

A8. Graph of heat flow against temperature for DSC analysis using spot specimen.

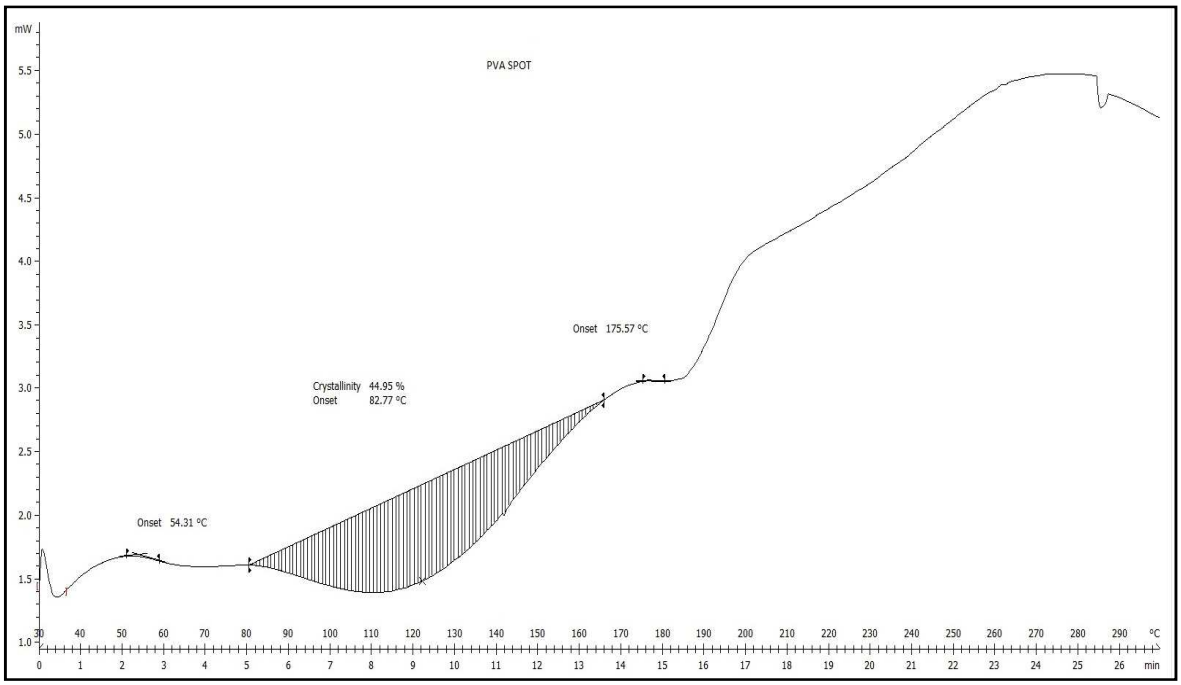

A9. Graph of heat flow against temperature for DSC analysis using no pattern (control) specimen.

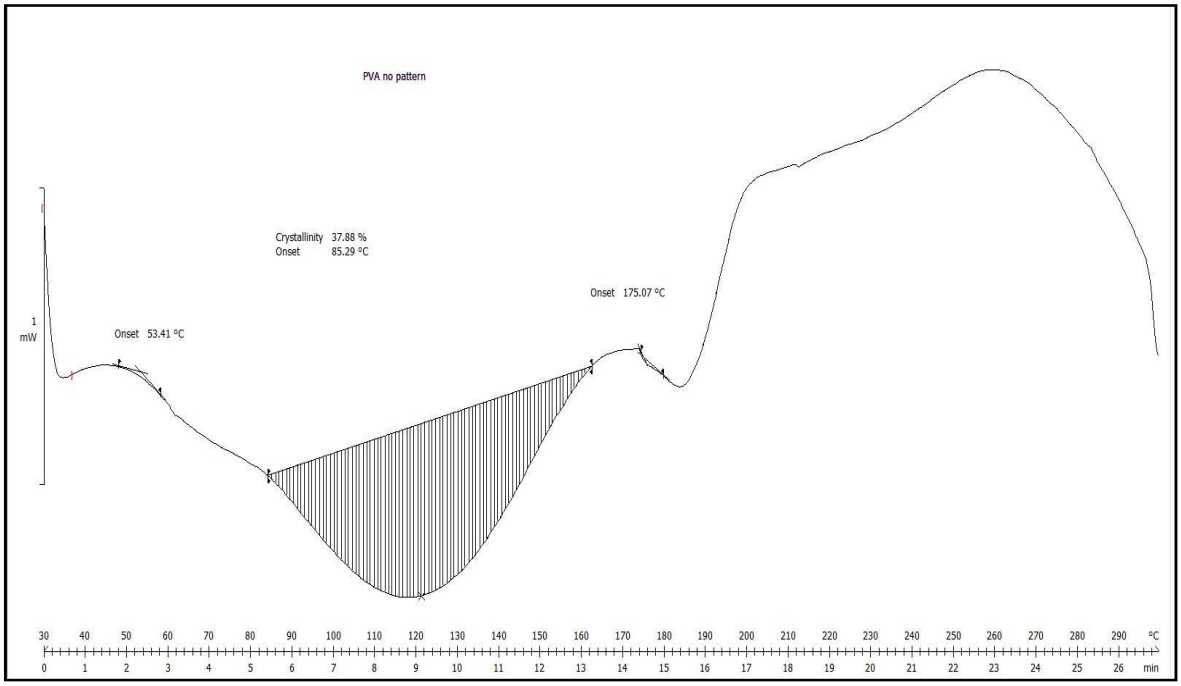

A10. Data for Loss modulus of PVA using Mettler Toledo DMA analyzer.

Loss Modulus of PVA **11.04.2013 10:45**

Curve Name:
=[]£PVA CLEAR, 11.04.2013 10:42:55
Curve Values:

Index	t [s]	x value [Hz]	y value [MPa]
0	45	270	507.428
1	57	260	498.795
2	69	250	490.162
3	82	240	481.53
4	95	230	472.897
5	108	220	464.265
6	121	210	455.632
7	134	200	448.193
8	146	190	440.6
9	159	180	433.445
10	172	170	426.805
11	185	160	420.669
12	197	150	415.308
13	210	140	409.53
14	223	130	403.776
15	236	120	397.482
16	248	110	389.736
17	260	100	380.863
18	273	90	372.915
19	286	80	361.621
20	299	70	345.149
21	311	60	331.525
22	323	50	317.901
23	336	40	304.276
24	349	30	290.652
25	361	20	277.028
26	374	10	263.403

Results:
Sample:
PVA CLEAR, Length 10.0000 mm, Width 6.1700 mm, Thickness 0.3400 mm, Geometry factor 4766.8984 1/m

Curve Name:
=[]£PVA STRIATION, 11.04.2013 10:42:55
Curve Values:

Index	t [s]	x value [Hz]	y value [MPa]
0	38	270	521.829
1	50	260	516.42
2	63	250	511.01
3	77	240	505.601
4	89	230	500.192
5	102	220	494.782
6	115	210	489.373
7	127	200	482.484
8	140	190	477.222
9	153	180	471.761
10	166	170	465.296
11	178	160	461.067
12	191	150	455.497
13	204	140	450.031
14	217	130	444.916
15	229	120	437.604
16	242	110	429.383
17	255	100	419.703
18	268	90	408.473
19	281	80	395.423
20	293	70	377.881
21	306	60	361.903
22	319	50	345.924
23	331	40	329.946
24	345	30	313.968
25	358	20	297.989
26	370	10	282.011

Results:
Sample:
PVA STRIATION, Length 10.0000 mm, Width 6.1700 mm, Thickness 0.3400 mm, Geometry factor 4766.8984 1/m

Curve Name:
=[]£PVA GRID, 11.04.2013 10:42:55
Curve Values:

Index	t [s]	x value [Hz]	y value [MPa]
0	40	270	548.314
1	53	260	543.973
2	65	250	539.631
3	78	240	535.289

4	91	230	530.948
5	104	220	526.606
6	117	210	522.264
7	130	200	518.494
8	143	190	514.962
9	155	180	510.954
10	168	170	506.654
11	182	160	503.127
12	195	150	499.821
13	207	140	496.91
14	220	130	493.959
15	233	120	489.02
16	245	110	481.142
17	258	100	471.04
18	270	90	461.026
19	284	80	448.032
20	297	70	429.958
21	310	60	412.782
22	322	50	395.606
23	335	40	378.431
24	347	30	361.255
25	360	20	344.079
26	373	10	326.903

Results:
Sample:
PVA GRID, Length 10.0000 mm, Width 6.1700 mm, Thickness 0.3400 mm, Geometry factor 4766.8984 1/m

Curve Name:
=[]£PVA DOTTED, 11.04.2013 10:42:55
Curve Values:

Index	t [s]	x value [Hz]	y value [MPa]
0	44	270	525.817
1	57	260	522.684
2	69	250	519.552
3	81	240	516.42
4	94	230	513.288
5	107	220	510.156
6	118	210	507.024
7	131	200	503.751
8	143	190	499.91
9	156	180	496.544
10	169	170	494.195
11	181	160	491.188
12	194	150	488.828

13	206	140	486.601
14	218	130	487.047
15	231	120	480.183
16	243	110	473.589
17	256	100	464.951
18	269	90	454.64
19	282	80	442.308
20	294	70	425.464
21	306	60	409.45
22	319	50	393.436
23	331	40	377.421
24	342	30	361.407
25	355	20	345.392
26	369	10	329.378

Results:
Sample:
PVA DOTTED, Length 10.0000 mm, Width 6.1700 mm, Thickness 0.3400 mm, Geometry factor 4766.8984 1/m

---

Not signed STARe SW 12.00

A11. Data for storage modulus of PVA using Mettler Toledo DMA analyzer.

Storage Modulus of PVA **12.04.2013 14:01**

Curve Name:
=[]£PVA GRID, 12.04.2013 13:59:43
Curve Values:

Index	t [s]	x value [Hz]	y value [MPa]
0	40	270	1331.63
1	53	260	1312.53
2	65	250	1293.44
3	78	240	1274.35
4	91	230	1255.25
5	104	220	1236.16
6	117	210	1217.06
7	130	200	1197.56
8	143	190	1178.08
9	155	180	1155.86
10	168	170	1132.47

11	182	160	1107.29
12	195	150	1081.56
13	207	140	1054.59
14	220	130	1024.06
15	233	120	991.762
16	245	110	958.184
17	258	100	920.737
18	270	90	881.156
19	284	80	835.205
20	297	70	782.33
21	310	60	730.367
22	322	50	678.404
23	335	40	626.441
24	347	30	574.479
25	360	20	522.516
26	373	10	470.553

Results:
Sample:
PVA GRID, Length 10.0000 mm, Width 6.1700 mm, Thickness 0.3400 mm, Geometry factor 4766.8984 1/m

Curve Name:
=[]£PVA STRIATION, 12.04.2013 13:59:44
Curve Values:

Index	t [s]	x value [Hz]	y value [MPa]
0	38	270	1172.29
1	50	260	1155.38
2	63	250	1138.47
3	77	240	1121.56
4	89	230	1104.65
5	102	220	1087.74
6	115	210	1070.83
7	127	200	1053.22
8	140	190	1034.32
9	153	180	1014
10	166	170	993.504
11	178	160	973.006
12	191	150	951.334
13	204	140	926.897
14	217	130	901.203
15	229	120	872.309
16	242	110	841.454
17	255	100	807.187
18	268	90	768.259
19	281	80	725.21

20	293	70	675.873
21	306	60	627.294
22	319	50	578.716
23	331	40	530.138
24	345	30	481.559
25	358	20	432.981
26	370	10	384.402

Results:
Sample:
PVA STRIATION, Length 10.0000 mm, Width 6.1700 mm, Thickness 0.3400 mm, Geometry factor 4766.8984 1/m

Curve Name:
=[]£PVA CLEAR, 12.04.2013 13:59:44
Curve Values:

Index	t [s]	x value [Hz]	y value [MPa]
0	45	270	1036.3
1	57	260	1020.88
2	69	250	1005.46
3	82	240	990.049
4	95	230	974.634
5	108	220	959.219
6	121	210	943.804
7	134	200	926.078
8	146	190	910.638
9	159	180	893.684
10	172	170	875.941
11	185	160	858.075
12	197	150	838.345
13	210	140	816.993
14	223	130	794.43
15	236	120	770.322
16	248	110	744.958
17	260	100	716.493
18	273	90	685.024
19	286	80	649.559
20	299	70	609.749
21	311	60	569.518
22	323	50	529.287
23	336	40	489.056
24	349	30	448.825
25	361	20	408.594
26	374	10	368.363

Results:
Sample:
PVA CLEAR, Length 10.0000 mm, Width 6.1700 mm, Thickness 0.3400 mm, Geometry factor 4766.8984 1/m

Curve Name:
=[]£PVA DOTTED, 12.04.2013 13:59:44
Curve Values:

Index	t [s]	x value [Hz]	y value [MPa]
0	44	270	1351.85
1	57	260	1333.43
2	69	250	1315.02
3	81	240	1296.6
4	94	230	1278.18
5	107	220	1259.76
6	118	210	1241.35
7	131	200	1221.79
8	143	190	1202.38
9	156	180	1181.6
10	169	170	1157.6
11	181	160	1134.71
12	194	150	1110.53
13	206	140	1084.03
14	218	130	1053.42
15	231	120	1020.53
16	243	110	985.169
17	256	100	947.792
18	269	90	907.667
19	282	80	860.913
20	294	70	806.62
21	306	60	753.743
22	319	50	700.867
23	331	40	647.99
24	342	30	595.114
25	355	20	542.237
26	369	10	489.361

Results:
Sample:
PVA DOTTED, Length 10.0000 mm, Width 6.1700 mm, Thickness 0.3400 mm, Geometry factor 4766.8984 1/m

A12. Data for Tan delta of PVA using Mettler Toledo DMA analyzer.

Tan Delta for PVA **11.04.2013 10:54**

Curve Name:
=[]£PVA CLEAR
Curve Values:

Index	t [s]	x value [Hz]	y value []
0	45	270	0.489549
1	57	260	0.488374
2	69	250	0.4872
3	82	240	0.486025
4	95	230	0.484851
5	108	220	0.483676
6	121	210	0.482502
7	134	200	0.484297
8	146	190	0.484353
9	159	180	0.485649
10	172	170	0.48812
11	185	160	0.491779
12	197	150	0.497427
13	210	140	0.503923
14	223	130	0.511649
15	236	120	0.520232
16	248	110	0.528169
17	260	100	0.537383
18	273	90	0.552676
19	286	80	0.568249
20	299	70	0.583328
21	311	60	0.601174
22	323	50	0.61902
23	336	40	0.636867
24	349	30	0.654713
25	361	20	0.672559
26	374	10	0.690405

Results:
Sample:
PVA CLEAR, Length 10.0000 mm, Width 6.1700 mm, Thickness 0.3400 mm, Geometry factor 4766.8984 1/m

Curve Name:
=[]£PVA STRIATION
Curve Values:

Index	t [s]	x value [Hz]	y value []
0	38	270	0.444149
1	50	260	0.446378
2	63	250	0.448607
3	77	240	0.450836
4	89	230	0.453066
5	102	220	0.455295
6	115	210	0.457524
7	127	200	0.458815
8	140	190	0.462231
9	153	180	0.466206
10	166	170	0.469385
11	178	160	0.475483
12	191	150	0.480851
13	204	140	0.488176
14	217	130	0.497352
15	229	120	0.506329
16	242	110	0.51648
17	255	100	0.527993
18	268	90	0.541637
19	281	80	0.560769
20	293	70	0.580907
21	306	60	0.601397
22	319	50	0.621886
23	331	40	0.642375
24	345	30	0.662865
25	358	20	0.683354
26	370	10	0.703843

Results:
Sample:
PVA STRIATION, Length 10.0000 mm, Width 6.1700 mm, Thickness 0.3400 mm, Geometry factor 4766.8984 1/m

Curve Name:
=[]£PVA GRID
Curve Values:

Index	t [s]	x value [Hz]	y value []
0	40	270	0.410217
1	53	260	0.413493
2	65	250	0.416769
3	78	240	0.420045

4	91	230	0.423321
5	104	220	0.426598
6	117	210	0.429874
7	130	200	0.434017
8	143	190	0.438334
9	155	180	0.443608
10	168	170	0.449525
11	182	160	0.45704
12	195	150	0.465014
13	207	140	0.47493
14	220	130	0.487197
15	233	120	0.498556
16	245	110	0.508222
17	258	100	0.518592
18	270	90	0.531808
19	284	80	0.547938
20	297	70	0.566429
21	310	60	0.583696
22	322	50	0.600962
23	335	40	0.618228
24	347	30	0.635495
25	360	20	0.652761
26	373	10	0.670028

Results:
Sample:
PVA GRID, Length 10.0000 mm, Width 6.1700 mm, Thickness 0.3400 mm, Geometry factor 4766.8984 1/m

Curve Name:
=[]£PVA DOTTED
Curve Values:

Index	t [s]	x value [Hz]	y value []
0	44	270	0.387705
1	57	260	0.391291
2	69	250	0.394877
3	81	240	0.398463
4	94	230	0.402049
5	107	220	0.405635
6	118	210	0.409221
7	131	200	0.413234
8	143	190	0.416733
9	156	180	0.421547
10	169	170	0.428458
11	181	160	0.43475
12	194	150	0.442706

13	206	140	0.452399
14	218	130	0.468009
15	231	120	0.476817
16	243	110	0.487713
17	256	100	0.497991
18	269	90	0.509873
19	282	80	0.524894
20	294	70	0.543541
21	306	60	0.560437
22	319	50	0.577333
23	331	40	0.594229
24	342	30	0.611126
25	355	20	0.628022
26	369	10	0.644918

Results:
Sample:
PVA DOTTED, Length 10.0000 mm, Width 6.1700 mm, Thickness 0.3400 mm, Geometry factor 4766.8984 1/m

---

Not signed STARe SW 12.00